Journal of Multiscale Modelling
Vol. 3, No. 4 (2011) 1–42

DOI: 10.1142/S1756973711000509

Imperial College Press
www.icpress.co.uk

MULTISCALE CONTINUOUS AND DISCONTINUOUS MODELING OF HETEROGENEOUS MATERIALS: A REVIEW ON RECENT DEVELOPMENTS

VINH PHU NGUYEN*,§, MARTIJN STROEVEN†
and LAMBERTUS JOHANNES SLUYS‡

Delft University of Technology
Faculty of Civil Engineering and Geosciences
P. O. Box 5048, 2600 GA Delft, The Netherlands
**V.P.Nguyen@tudelft.nl*
†*M.Stroeven@tudelft.nl*
‡*L.J.Sluys@tudelft.nl*

This paper reviews the recent developments in the field of multiscale modelling of heterogeneous materials with emphasis on homogenization methods and strain localization problems. Among other topics, the following are discussed (i) numerical homogenization or unit cell methods, (ii) continuous computational homogenization for bulk modelling, (iii) discontinuous computational homogenization for adhesive/cohesive crack modelling and (iv) continuous-discontinuous computational homogenization for cohesive failures. Different boundary conditions imposed on representative volume elements are described. Computational aspects concerning robustness and computational cost of multiscale simulations are presented.

Keywords: Homogenization; computational homogenization; representative volume element (RVE); multiscale; crack; strain localization; damage; heterogeneous materials.

1. Introduction

Many natural and engineering materials such as rock, concrete, metal, fiber-reinforced composites etc. have a heterogeneous structure at a certain level of observation. These materials are often referred to as *composite materials* or *multi-phase materials* or *heterogeneous materials*. In this paper, composite is usually used to indicate two-phase materials with a regular structure. From an engineering point of view, heterogeneous materials are desirable because they can be tailor made to take advantage of particular properties of each constituent. For example, fiber reinforced concrete is concrete containing fibrous material in which fibers are usually used to control cracking.

It has been widely recognized that many macroscopic phenomena originate from the mechanics of the underlying microstructure. The size, shape, spatial

§Corresponding author.

distribution, volume fraction and properties of the constituents making up the microstructure all have a significant impact on the behavior of the material observed at the macroscale. Furthermore, external loading applied on the materials at the macroscale might in turn change the microstructural morphology e.g., void formation and coalescence in metals, cracking in cement matrix and interfacial transition zone in concrete.

Finding the relation between microstructure and macroscopic properties (in short *structure-properties* relation) is an essential problem confronting material scientists as well as the computational mechanics community for decades. Such relations, if found, might have a strong impact in many engineering fields. This is because (i) the macroscopic behavior is much better captured compared to a prediction based on phenomenological constitutive models and (ii) it provides an alternative to design new materials of which desired macroscopic properties can be obtained by adjusting the underlying microstructure. It is emphasized that the development of new materials is basically done empirically, that is, a large number of specimens with different microstructures are fabricated and tested, until specific requirements on the behavior are fulfilled. Obviously, computational models are preferable over this time consuming and expensive empirical method.

Brute-force approaches in which the microstructure is explicitly taken into account at the coarse scale model are practically not feasible due to the prohibitive computational expense they would lead to. Therefore, over the years, a number of analytical/numerical models, that are usually referred to as *multiscale models* have been developed. These models are based on the physics of microstructures, which are able to predict, in an efficient manner, the macroscopic behavior of heterogeneous materials. In this paper, the terminology "multiscale" should be understood as multiple length scales. The term "multiscale method" indicates a formulation in which multiple length scales are resolved and there is an exchange of information between the length scales.

Traditionally multiscale modeling of heterogeneous materials is performed either within the framework of *homogenization methods* for problems in which the scales are clearly separated or within the framework of *concurrent methods* when the scales are coupled. The discussion is restricted to continuum/continuum coupling. For atomistic/continuum coupling i.e., MD-FEM coupling, we refer to an overview reported in Curtin and Miller[14] and for discrete/continuum coupling i.e., DEM-FEM coupling, see e.g., Refs. 4, 101, 113 and 153 and references therein where MD stands for molecular dynamics, FEM is short for finite element method and DEM is for discrete element method.

1.1. *Homogenization methods*

Homogenization is a method to determine the *apparent* or *overall* properties of a heterogeneous material thereby allowing one to substitute this material with an equivalent homogeneous material, see Fig. 1. Homogenization methods can

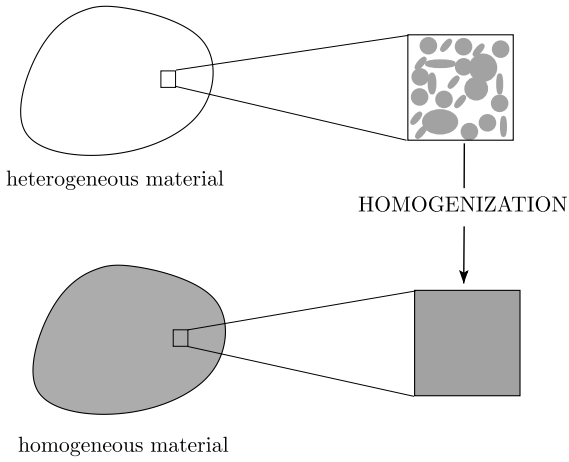

Fig. 1. Homogenization of a heterogeneous material. Based on Temizer and Zohdi.[141]

be divided into three categories namely analytical/mathematical homogenization, numerical homogenization and computational homogenization. In this paper, analytical/mathematical homogenization, albeit very useful in some circumstances, is left out of consideration since this technique is usually restricted to simple microscopic geometries and material models (mostly at small strains). A comprehensive overview of analytical homogenization methods can be found in the textbook of Nemat-Nasser and Hori.[104]

In numerical homogenization schemes, a macroscopic canonical constitutive model e.g., a visco-plasticity model, is assumed with parameters determined by fitting the data produced by FE (or any other numerical method) computations of a microscopic sample where the microstructure is explicitly modeled. In the literature, those numerical homogenization techniques are known as unit cell methods, we refer to Christman *et al.*,[11] Nakamura and Suresh,[103] van der Sluis *et al.*,[146] Pettermann and Suresh,[123] among others, and references therein. Unit cell methods are particularly useful in modeling composite materials since they enable the development of the so-called homogenization-based or micromechanically derived continuum damage and plastic models[15,56,57,83,124] that can be used in structural computations. Due to the assumption on the form of the macroscopic constitutive law, the methods become less appropriate for nonlinear problems with evolving microstructures. On the other hand, these methods are computationally attractive for large scale computations since microscopic FE computations are conducted *a priori*.

In computational homogenization (CH) methods,[137] the macroscopic constitutive behavior is defined *on the fly* during simulation. Due to this flexibility, the methods have been utilized to predict mechanical behavior of materials having complex microstructures, see Guedes and Kikuchi,[39] Fish *et al.*,[26,27] Ghosh *et al.*,[32] Smit *et al.*,[130] Miehe *et al.*,[100] Feyel and Chaboche,[23] Kouznetsova *et al.*[68] among

others. Not only mechanical problems describing linear and nonlinear deformations but also thermal problems, see Özdemir *et al.*,[119] Monteiro *et al.*,[102] Larsson *et al.*[77] and multi-physics problems (thermo-mechanical in Özdemir *et al.*,[120] electro-mechanical in Schröder and Keip[128]) have recently been addressed with this method. Other applications encompass thin structures,[13,95,96,114,117] uncoupled consolidation in heterogeneous porous media[76] and solidification problems.[80] Computational homogenization models are also adopted in bioengineering, see e.g., Refs. 34 and 155. In Ricker *et al.*,[126,127] the classical CH scheme has been extended toward the homogenization of configurational quantities in the context of defect mechanics. A unified variational basis of CH theory for bulk materials has been recently presented in Perić *et al.*[122] Implementation of CH models in ABAQUS was presented in Yuan and Fish.[157]

1.2. *Concurrent methods*

The characteristic of concurrent methods is that the microstructural features are resolved directly on the macroscopic model. Two basic issues involved in this kind of method are (i) how to handle the coupling between the coarse scale mesh and the fine scale mesh and (ii) efficient algorithms for adaptive addition of fine scale features to the coarse scale model. Typical works on concurrent multiscale analysis of material failure are given in Guidault *et al.*,[40] Eckardt and Könke,[19] Lloberas-Valls *et al.*[86] which are based on domain decomposition methods and Hettich *et al.*,[44] Loehnert and Belytschko[87] which are based on the variational multiscale method.[52] Figure 2 gives some application examples of using concurrent models for failure analysis of heterogeneous materials. Another multiscale method with strong macro-micro coupling has been given in Ibrahimbegović and Markovič[54] for elasto-plastic multiphase materials and in Gitman *et al.*[35] for quasi-brittle softening materials. Multiscale methods that adaptively combine a (numerical) homogenization technique and a concurrent method have been presented in, among others, Ghosh *et al.*,[33] Larsson and Runesson,[75] Temizer and Wriggers[140] and references therein. A homogenized constitutive model (obtained via a numerical homogenization) is utilized for domains having benign deformations while a concurrent formulation is adopted in critical regions of high gradients where the macroscopic fields vary considerably. The Arlequin method developed by Dhia and Rateau[17] is yet another framework that can be used in concurrent multiscale analyses. Lim *et al.*[84] used variable-node finite elements to model a composite material. Variable-node elements serve as transition elements that link the standard four-noded quadrilateral elements to the domain in which the microstructure is explicitly meshed. The mesh superposition method (or the s-version of FEM) proposed by Fish[24] is used in Kawagai *et al.*[64] for multiscale modeling of complex and heterogeneous porous microstructures.

A numerical multiscale method for modeling fracture of heterogeneous quasi-brittle solids has been given in Kaczmarczyk *et al.*[60] where the designation

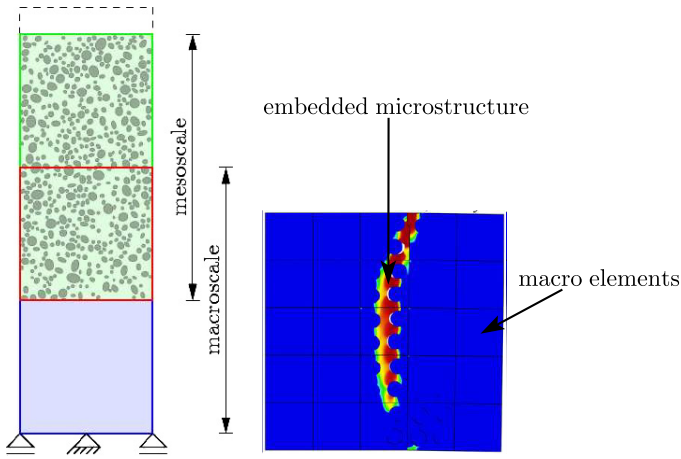

Fig. 2. Concurrent multiscale models based on: (a) overlapping domain decomposition method Eckardt and Könke[19] and (b) variational multiscale method Hettich *et al.*[44]

numerical is used to indicate the use of a multi-grid solution strategy, that utilizes scale transition techniques derived for computational homogenization pioneered by Miehe and Bayreuther,[98] to solve the very large system of algebraic equations that emerges from a detailed resolution of the fine-scale structure. This method can be viewed as a Direct Numerical Solution (DNS) with an efficient solution scheme.

1.3. *Aims and outline*

It should be mentioned that there exist excellent reviews on the subject of multiscale modeling of heterogeneous materials. Kanouté *et al.*[62] gave such a survey in 2009. However, the review was focused more on analytical/mathematical homogenization such as asymptotic homogenization methods, mean field approaches, transformation field analysis etc. A recent review of CH methods and applications has been given by Geers *et al.*[29] in 2010. A review of multiscale methods can also be found in the textbook of Fish.[25] The aim of this paper is to review recent developments in the field which have not been covered in Refs. 25 and 29 and 62. The survey focuses on multiscale models for localization problems. Among other topics, the following are discussed: (i) numerical homogenization or unit cell methods, (ii) continuous computational homogenization for bulk modeling, (iii) discontinuous computational homogenization for adhesive/cohesive crack modeling and (iv) continuous-discontinuous computational homogenization for cohesive failures. Also presented are commonly used boundary conditions and the issue of existence of representative volume elements (RVE). The manuscript presents the current trends in computational homogenization for heterogeneous materials. Unresolved issues

are identified. Since homogenization is such a huge field of constant progresses, if any paper is not discussed here, it is simply due to our limited knowledge.

The remainder of the paper is structured as follows. Section 2 presents the essential features of the continuous computational homogenization model. Section 3 discusses some hybrid homogenization methods that combine numerical homogenization and computational homogenization. In Sec. 4, discontinuous homogenization methods for modeling adhesive and cohesive failure are given. Section 5 is dedicated to the so-called continuous-discontinuous computational homogenization methods for multiscale modeling of cracks. Computational aspects are given in Sec. 6 followed by a discussion on computational homogenization in a dynamics context in Sec. 7. Section 8 concludes the paper by pointing out some potential future research directions.

2. Continuous Computational Homogenization Model

This section briefly presents the continuous computational homogenization method. Through this, basic concepts of CH methods are discussed. The material given in this section is required in developing enhanced discontinuous and continuous-discontinuous CH schemes, to be presented in subsequent sections, for strain localization and failure phenomena.

2.1. *General procedure*

Continuous CH methods are utilized to define on the fly the macroscopic stress-strain relation $\boldsymbol{\sigma}_{\mathrm{M}} - \boldsymbol{\epsilon}_{\mathrm{M}}$ for a macroscopic point from a microscopic sample attached to this point. That is why CH is also referred to as *multiscale constitutive modeling*. All the heterogeneities of the underlying microstructure are explicitly resolved in the microscopic sample. The behavior of the microstructural constituents are modeled by classic phenomenological constitutive laws.

The procedure is given in Fig. 3 which can be briefly described as follows. For a point (e.g., an integration point in the spatially discretized macroscopic solid) in the macro-solid with a strain $\boldsymbol{\epsilon}_{\mathrm{M}}$, instead of inserting this strain into a (phenomenological) constitutive box to obtain the corresponding stress $\boldsymbol{\sigma}_{\mathrm{M}}$, the strain is used as a boundary condition imposed on the external boundary Γ_{m} of the microscopic sample Ω_{m} with size l_{m}. The equilibrium of this micro-sample is obtained after solving the microscopic boundary value problem (BVP). The macroscopic stresses $\boldsymbol{\sigma}_{\mathrm{M}}$ are then defined as the volume average of the microscopic stresses over the micro-sample. When implemented in a finite element (FE) framework, the method is known as an FE^2 scheme.[21] The discussion here is confined to two-dimensional quasi-static problems. For a treatment of computational homogenization in a three-dimensional dynamic setting, we refer to Refs. 63 and 155. A comprehensive treatment of the CH theory in the finite deformation regime is given in the dissertation of Kouznetsova[67] (see also the work of Ref. 16). Grytz and Meschke[38] presented a finite deformation CH theory in curvilinear convected coordinates for realistic

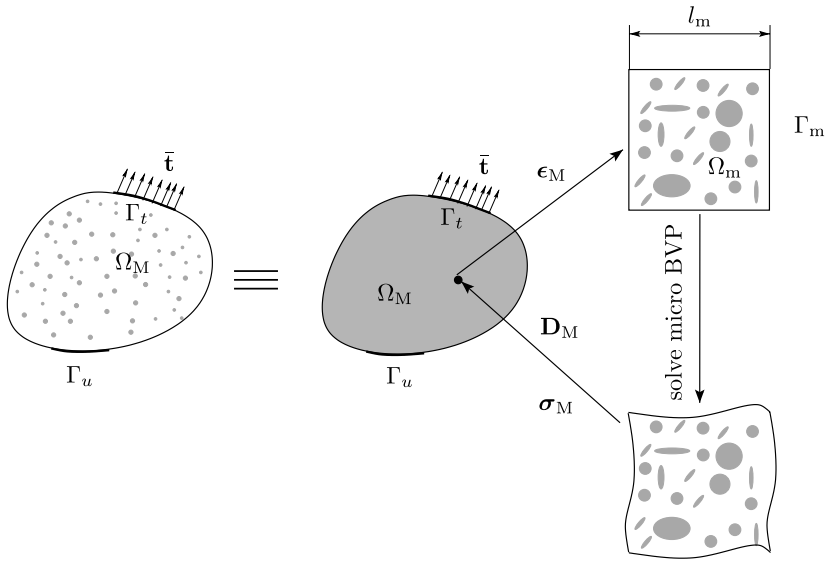

Fig. 3. Multiscale modelling of a heterogeneous solid with the continuous/bulk computational homogenization scheme.

biomechanical multi-scale simulations of shell-like soft tissues. Note that standard CH models would require different RVEs at each macroscopic point (one single RVE is rotated according to the curvilinear path of the physical material directions at the macro-scale). In contrast, Grytz and Meschke[38] introduced different physical spaces at micro- and macro-scale, the same initial RVE can therefore be used for every macroscopic point.

Given a macroscopic strain vector $\boldsymbol{\epsilon}_{\mathrm{M}}$ of an integration point (also called Gauss point (GP) in this paper), one is seeking for the corresponding macroscopic stress vector $\boldsymbol{\sigma}_{\mathrm{M}}$ and the macroscopic material tangent $\mathbf{D}_{\mathrm{M}}$. The procedure, usually referred to as *a multiscale constitutive box*, is given in Box 1.

Box 1 Procedure of the continuous CH scheme (at level of macroscopic integration points).

(1) **Downscaling** or macro-to-micro transition. The macroscopic strain vector $\boldsymbol{\epsilon}_{\mathrm{M}}$ is transformed to the RVE as boundary conditions. Note that the specific BCs must fulfill the **strain averaging theorem**.
(2) The BVP of the RVE (in short, the micro-BVP) is solved.
(3) **Upscaling** or micro-to-macro transition. The microscopic stresses are upscaled to the macroscale as the macroscopic stress vector. This is achieved based on the **Hill–Mandel principle**. Besides, the microscopic stiffness matrix is upscaled to the macroscopic material tangent $\mathbf{D}_{\mathrm{M}}$.

2.2. *Basic ingredients of CH theory*

The theory of homogenization is based on the following ingredients

- Existence of a Representative Volume Element (RVE)
- Principle of separation of scales
- Averaging theorem e.g., strain and stress averaging theorems
- The Hill–Mandel macro-homogeneity principle
- Availability of constitutive behavior of RVE's constituents.

For the subsequent discussion an assumption was made of the existence of such an RVE. In the following discussion, for simplicity, it has been assumed that the RVE does not contain cracks. Furthermore, voids, if present in the RVE, are traction-free i.e., the traction vanishes on the surfaces of the voids. Relaxation of the first assumption was made in for example Zohdi and Wriggers[162] whereas the extension of the CH theory to the case in which the second assumption is relaxed has been given in Perić *et al.*[122]

2.2.1. *Existence of a representative volume element*

In homogenization methods, the macroscopic response is defined as the average of the response of a microscopic sample with a finite size in which the microstructure is explicitly resolved. This microscopic sample is referred to as *unit cell* for materials with an ordered microstructure, see left part of Fig. 4, and as RVE (this concept was introduced by Hill[45]) for materials having a random microstructure, see right part of Fig. 4. Other names including Microstructural Volume Element (MVE), Statistically Equivalent RVE (SERVE) are also used for this microscopic sample.

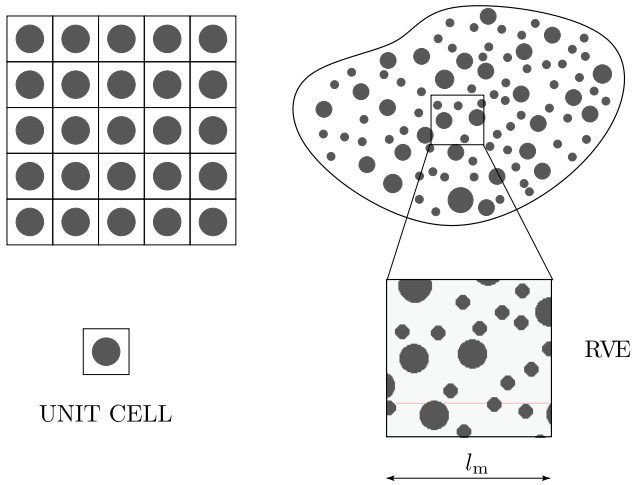

Fig. 4. Representative volume element for an ordered/structured composite material (left) and for a disordered/random material (right).

In brief, the RVE corresponds to a microstructural subdomain that is representative of the entire microstructure in an average sense.

In general, the size of an RVE of a material depends on

- the sought for effective properties;
- the loading conditions;
- the boundary conditions imposed on the RVE;
- whether strain localization occurs.

The existence of an RVE and its size for random heterogeneous materials have been addressed by several authors, see e.g., Refs. 18, 36, 61, 108, 118, 121, 136, 138 and 139 and references therein. Gitman *et al.*[36] did an interesting study on the existence of an RVE for quasi-brittle heterogeneous materials that exhibit localization of deformation. They found that an RVE does not exist for such materials since the material loses its statistical homogeneity upon strain localization. Recently, Nguyen *et al.*,[108] via the *failure zone averaging scheme*, showed that there exists an RVE for quasi-brittle heterogeneous materials exhibiting strain localization if a traction-separation relation, not a stress-strain relation, is the homogenized property.

In a CH scheme, a microscopic sample is said to be an RVE when the following conditions are satisfied

- an increase in its size (of the same structural realization) does not lead to considerable differences in the homogenized properties;
- its size is much smaller than the characteristic length l_{M} over which the macroscopic loading varies in space, $l_{\mathrm{m}} \ll l_{\mathrm{M}}$. This condition is known as the principle of separation of scales.

2.2.2. *Principle of separation of scales*

According to Geers *et al.*,[29] the principle of separation of scales is formulated as follows: "*The microscopic length scale* l_{m} *is assumed to be much smaller than the characteristic length* l_{M} *over which the macroscopic loading varies in space*". That is,

$$l_{\mathrm{m}} \ll l_{\mathrm{M}} \tag{1}$$

which requires the RVE to be sufficiently small so that the macroscopic fields (stress or strain) are uniform over it. Since the RVE's volume is small ($\Omega_{\mathrm{m}} = \mathcal{O}(l_{\mathrm{m}}^3)$), the inertial and body forces can be neglected at the microscale. Therefore the general dynamic equilibrium of the RVE reduces to the static equilibrium that reads $\boldsymbol{\nabla} \cdot \boldsymbol{\sigma}_{\mathrm{m}} = \mathbf{0}$ in Ω_{m} where $\boldsymbol{\sigma}_{\mathrm{m}}$ denotes the microscopic stresses.

2.2.3. *Strain averaging theorem*

The strain at any point $\mathbf{x}_{\mathrm{M}}$ in the macroscopic solid is defined as the volume average of the microscopic strain $\boldsymbol{\epsilon}_{\mathrm{m}}$ over the RVE that is associated with that point. That

is at any instant t,

$$\boldsymbol{\epsilon}_{\mathrm{M}}(\mathbf{x}_{\mathrm{M}}, t) = \frac{1}{|\Omega_{\mathrm{m}}|} \int_{\Omega_{\mathrm{m}}} \boldsymbol{\epsilon}_{\mathrm{m}}(\mathbf{x}_{\mathrm{m}}, t) \mathrm{d}\Omega \tag{2}$$

where $|\cdot|$ denotes the measure of the domain e.g., the area in two dimensions and the volume in three dimensions.

2.2.4. *Hill–Mandel macro-homogeneity principle*

Based on physical arguments, the Hill–Mandel macro-homogeneity principle[46,88] establishes that the macroscopic stress power must equal the volume average of the microscopic stress power over the RVE. That is, at any state of the RVE characterized by a stress field $\boldsymbol{\sigma}_{\mathrm{m}}$ in equilibrium,

$$\boldsymbol{\sigma}_{\mathrm{M}} : \dot{\boldsymbol{\epsilon}}_{\mathrm{M}} = \frac{1}{|\Omega_{\mathrm{m}}|} \int_{\Omega_{\mathrm{m}}} \boldsymbol{\sigma}_{\mathrm{m}} : \dot{\boldsymbol{\epsilon}}_{\mathrm{m}} \mathrm{d}\Omega \tag{3}$$

must hold for any $\dot{\boldsymbol{\epsilon}}_{\mathrm{m}}$. The symbol: indicates the double contraction operator when applied for two second order tensors $\mathbf{A}$ and $\mathbf{B}$ yields $\mathbf{A}$:$\mathbf{B} = A_{ij}B_{ij}$.

By substituting a specific boundary condition that fulfills the strain averaging theorem given in Eq. (2) into Eq. (3), one obtains

$$\boldsymbol{\sigma}_{\mathrm{M}}(\mathbf{x}_{\mathrm{M}}, t) = \frac{1}{|\Omega_{\mathrm{m}}|} \int_{\Omega_{\mathrm{m}}} \boldsymbol{\sigma}_{\mathrm{m}}(\mathbf{x}_{\mathrm{m}}, t) \mathrm{d}\Omega \tag{4}$$

This indicates that the macroscopic stress tensor is defined as the volume average of the microscopic stress tensor.

2.2.5. *Availability of constitutive behavior of RVE's constituents*

Although the constitutive behavior of the material at the macroscale is not needed *a priori* in a CH framework, the behavior of the microstructural constituents must be identified prior to the simulation. This can be achieved with phenomenological constitutive models of which parameters are determined using conventional parameter identification processes e.g., experiments and/or inverse analysis (see e.g., Ref. 53 and references therein) but now applied for individual microstructural constituents. Alternatively, constitutive models for the microscale phases can be defined using a numerical homogenization procedure or even a computational homogenization scheme by going one more scale down.

Remark 2.1. In contrast to mathematical homogenization that is based on the assumption of global periodicity, see Fig. 5, CH only assumes a local periodicity of the microstructure. This allows the modeling of effects of non-uniformity of microstructure on the macroscopic response as e.g., in functionally graded materials.

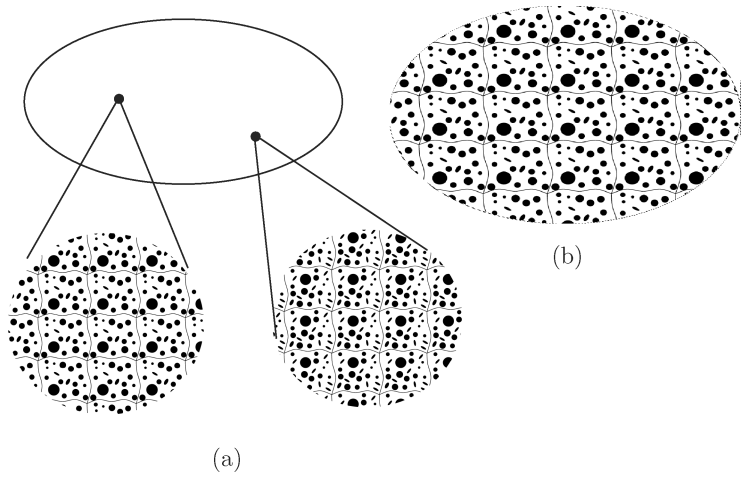

Fig. 5. Illustration of the concept of (a) local and (b) global periodicity.

2.3. *Boundary conditions*

An important aspect in RVE-based homogenization methods is the choice of boundary conditions (BCs), which are imposed on the RVE's boundary, used to capture the effect of the surrounding medium. The choice of BCs affects the result of homogenization methods including homogenized properties i.e., macroscale constitutive response, the required size of the RVE and the type (and extent) of localized failure taking place at the microscale. To the best knowledge of the authors, the following boundary conditions are commonly used in CH schemes

- Taylor BCs
- Linear BCs
- Constant traction BCs
- Periodic BCs
- Minimal kinematic BCs

Table 1 gives a summary of those BCs, see Fig. 6 for notations. More BCs will be presented when discontinuous homogenization methods are discussed. In literature, other BCs are also adopted such as the mixed-uniform BCs presented by Hazanov and Huet.[43] Mixed-uniform BCs, sometimes called mixed BCs, refer to the use of linear BCs on some parts of the RVE boundary and constant traction BCs on the remaining part. In Refs. 4 and 9, this BC is also adopted. The Taylor BC yields a homogeneous microscopic strain field i.e., there is no interaction between heterogeneities. This BC is therefore unrealistic and left out of consideration. Many authors[61,142,146] have proved that even for non-periodic heterogeneous materials, periodic BCs provide reasonable estimates of the effective properties. Compared to linear and constant traction BCs, periodic BCs give a faster convergence of the

Table 1. Commonly used boundary conditions for RVEs.

Name	Equation	Location	Localization
Taylor BCs	$\mathbf{u}_{\mathrm{m}}(\mathbf{x}) = \boldsymbol{\epsilon}_{\mathrm{M}} \cdot \mathbf{x}$	$\mathbf{x} \in \Omega_{\mathrm{m}}$	$-$
Linear BCs	$\mathbf{u}_{\mathrm{m}}(\mathbf{x}) = \boldsymbol{\epsilon}_{\mathrm{M}} \cdot \mathbf{x}$	$\mathbf{x} \in \Gamma_{\mathrm{m}}$	$-$
Constant traction BCs	$\mathbf{t}_{\mathrm{m}}(\mathbf{x}) = \boldsymbol{\sigma}_{\mathrm{M}} \cdot \mathbf{n}$	$\mathbf{x} \in \Gamma_{\mathrm{m}}$	$+$
Periodic BCs	$\mathbf{u}_{\Gamma^+_{\mathrm{m},2}} - \mathbf{u}_{\Gamma^-_{\mathrm{m},2}} = \mathbf{u}_4 - \mathbf{u}_1$		
	$\mathbf{u}_{\Gamma^+_{\mathrm{m},1}} - \mathbf{u}_{\Gamma^-_{\mathrm{m},1}} = \mathbf{u}_2 - \mathbf{u}_1$		$+$
	$\mathbf{u}_q = \boldsymbol{\epsilon}_{\mathrm{M}} \cdot \mathbf{x}_q, q = 1, 2, 4$		
Minimal kinematic BCs	$2\left\|\Omega_{\mathrm{m}}\right\| \epsilon^{\mathrm{M}}_{ij} = \int_{\Gamma_{\mathrm{m}}} (u_i n_j + u_j n_i) \mathrm{d}\Gamma$		$+$
	$\mathbf{u}_1 = \mathbf{0}, u^y_2 = 0$		

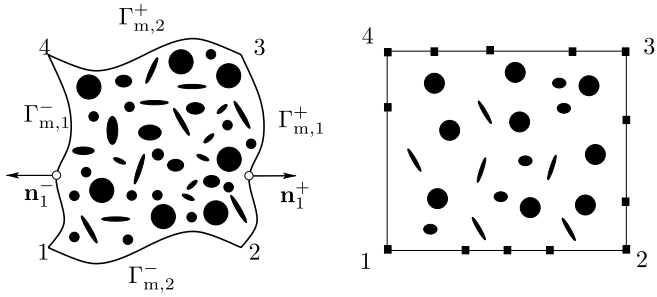

Fig. 6. Periodic representative volume element (left) and non-periodic RVE (right).

effective properties i.e., smaller RVEs can be used with periodic BCs. Periodic BCs are therefore probably the most commonly used boundary conditions for RVEs to date. For RVEs with strain localization, linear BCs should not be used as shown in Fig. 7 since they prevent localization bands or cracks from approaching the RVE boundary.

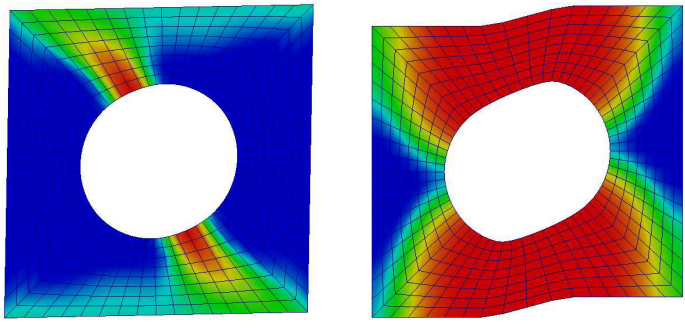

Fig. 7. A softening unit cell in shear: linear BCs prevent damage from occurring at the RVE boundary (left) while periodic BCs allows this (right). The contour plot shows the damage profile.

In Ref. 97, the authors argue that periodic BCs impose unphysical constraints on the unit cell, for example periodic BCs result in a stiffer constitutive response under shear loading. They propose the use of Minimal Kinematic (MK) BCs, in which the macroscopic loading is satisfied in a weak sense through a boundary integral, rather than at every point in the material domain. Inglis *et al.*[55] presents a comparative study of periodic and MKBCs for RVEs with interfacial debonding between the matrix and the inclusions. They concluded that the MKBCs provide the advantage of not requiring periodic RVE meshes; other than that localization zones obtained with both BCs are comparable. Other discussions on different BCs applied to the RVE can be found in Huet,[51] Hori and Nemat-Nasser.[50] Generally the advantages of one BC over the other diminish when increasing the size of RVEs. Note however that, in a CH-based simulation, small RVEs are preferable.

For two dimensional rectangular RVEs, the MKBCs read

$$\begin{aligned} |\Omega_{\mathrm{m}}|\,\epsilon_{\mathrm{M}}^{11} &= \int_{23} u_x \mathrm{d}y - \int_{41} u_x \mathrm{d}y \\ |\Omega_{\mathrm{m}}|\,\epsilon_{\mathrm{M}}^{22} &= -\int_{12} u_y \mathrm{d}x + \int_{34} u_y \mathrm{d}x \\ 2\,|\Omega_{\mathrm{m}}|\,\epsilon_{\mathrm{M}}^{12} &= -\int_{12} u_x \mathrm{d}x + \int_{23} u_y \mathrm{d}y + \int_{34} u_x \mathrm{d}x - \int_{41} u_y \mathrm{d}y \end{aligned} \tag{5}$$

we refer to Fig. 6 for notations. For RVEs subjected to linear, periodic and minimal kinematic BCs, the discrete equations of the RVE equilibrium read

$$\mathbf{f}_{\mathrm{int}}(\mathbf{u}_{\mathrm{m}}) = \mathbf{0} \tag{6}$$

$$\mathbf{C}\mathbf{u}_b = \mathbf{b}(\boldsymbol{\epsilon}_{\mathrm{M}}) \tag{7}$$

where $\mathbf{u}_{\mathrm{m}}$ are the microscopic nodal displacements, $\mathbf{f}_{\mathrm{int}}$ denotes the microscopic internal force vector, $\mathbf{C}$ is a constraint matrix, $\mathbf{u}_b$ represents the displacements of nodes residing on the RVE boundary and $\mathbf{b}(\boldsymbol{\epsilon}_{\mathrm{M}})$ is the applied BCs vector.

2.4. *Limitation of continuous CH applied for softening materials*

When strain localization occurs at the RVE level, the homogenized constitutive equation $\boldsymbol{\sigma}_{\mathrm{M}}-\boldsymbol{\epsilon}_{\mathrm{M}}$ is a strain softening constitutive equation. The severe consequence of this is that the macroscopic BVP is ill-posed or in mathematical terms, the macroscopic BVP loses ellipticity. Therefore, the numerical solution obtained with CH theory when softening materials are adopted at the microscale is sensitive with respect to the macroscopic finite element discretization. This has been shown in Gitman *et al.*[35] and recently in Bažant,[6] where the author has even questioned the applicability of the standard/conventional CH theory for softening materials.

One of the basic assumptions in homogenization theory is the existence of a representative volume element. It means that when using a microscopic sample which is larger than the RVE, the macroscopic response should remain unchanged.

As shown in Ref. 36, this is the case for non-softening materials but not for softening materials since the material loses statistical homogeneity upon strain localization. In summary, when applied to softening materials, the continuous/bulk CH theory suffers from two problems namely (i) the macroscopic BVP is ill posed and (ii) the method is not objective with respect to the size of the RVE.

In recent years attempts have been made to overcome the aforementioned drawbacks of continuous CH schemes for softening materials. They include the second-order CH scheme presented in Kouznetsova *et al.*,[69] the continuous-discontinuous CH schemes (see Refs. 90, 94–96) for masonry materials, and Ref. 112 for random heterogeneous materials,[134] for viscoelastic heterogeneous materials), the Multiscale Aggregating Method (MAD) presented in Belytschko *et al.*,[10] Belytschko and Song[9] and the discontinuous CH scheme for crack homogenization for random heterogeneous materials.[109,110,148,149] The coupled-volume method[35] also yields a response that is insensitive to the macroscopic FE mesh and RVE size. However, no discontinuities are introduced at macroscale.

Remark 2.2. The continuous CH scheme given in Fig. 3 is classified as a *first-order* (i.e., only the first gradient of the macroscopic displacement field is transferred to the microscale) homogenization scheme according to Kouznetsova *et al.*[69] in which the authors have presented a *second-order* CH method. Salient features of the second-order CH model are (i) a high order continuum model is employed at macroscale, (ii) first and second gradients of the macroscopic displacement field are used for the BCs imposed on the RVE and utilization of the generalized Hill–Mandel principle to define the macroscopic high order stresses. We refer to Kouznetsova *et al.*,[70] Larsson and Diebels,[79] Kaczmarczyk *et al.*[58,59] and references therein for recent studies on the second-order CH method. Compared to first-order CH schemes, the second-order CH model can model microstructural size effects and to some extent macroscopic localization. Moreover, they are very useful for homogenization of shells and beams. However, second-order CH schemes cannot properly deal with softening materials exhibiting deformation beyond a quadratic nature in the displacements.[29] A discussion of the RVE in the context of the second-order CH scheme was given in Kouznetsova *et al.*[71]

3. Other Homogenization Models

It is obvious that FE^2 methods are very computationally expensive, thus they are rarely used in large scale computations. Approximate multiscale constitutive models, which are derived from accurate micromechanical analyses, are preferable in structural computations. To this end, models that combine the best of numerical homogenization and computational homogenization have recently appeared in literature. The basic steps involved in these models are (i) *preliminary computations* wherein a large number of FE analyses realized on an RVE subjected to a wide range of possible straining is conducted, (ii) *construction of an effective constitutive law* in which the data obtained from step (i) are used to derive an effective stress-strain

relation and (iii) *macroscale computation* wherein whenever a stress-strain relation is required, the one in step (ii) is used rather than resorting to microscale computations. It should be emphasized that these models can be considered as *extended numerical homogenization models* wherein a postulation of the form of constitutive response at macroscale is bypassed.

Yvonnet *et al.*[161] presented such a model for nonlinear elastic heterogeneous materials. The strain space is discretized into a number of nodes. For each node in the strain space, a microscale FE computation is performed and an effective potential energy function is then computed. After this step, a discrete space of potential energy is obtained. During the structural computation, at a Gauss point with a given strain, the corresponding potential energy is obtained by interpolation of the discrete potential energy functions.

Artificial neural network (ANN) has been used to define approximate constitutive behavior, see e.g., Refs. 30 and 159 and references therein. Recently in the works of Unger and Könke[144,145] a homogenization scheme using an ANN was presented. The basic idea is to combine numerical homogenization (efficient but restricted) and computational homogenization (general but expensive) into one common framework. To this end, an ANN is used as a material model on the macroscale. The ANN is trained using microscale simulations. The proposed homogenization scheme was used in a multiscale analysis of a reinforced concrete beam. We refer to Lefik *et al.*,[81] Hambli[42] for related discussions on ANN and homogenization.

A hybrid numerical-computational homogenization method was described in Andrade and Tu[4] for granular materials. For numerical homogenization, a phenomenological plasticity model is assumed for the macroscopic behavior. For computational homogenization, some key parameters of the plasticity model are computed on the fly by resorting to microscale computations. More precisely, during the macroscopic analysis, for an integration point, a strain is transferred to a unit cell (where a discrete element formulation is used to model the grains); the unit cell DEM problem is solved and the dilatancy and frictional resistance are upscaled to that integration point. Then, a standard return mapping algorithm can be used at macroscale to compute the stresses and the consistent tangent. A recent paper on this method can be found in Andrade *et al.*[5]

For completeness, the multiscale continuum theory (also known as the multiscale micromorphic theory) presented in McVeigh *et al.*,[93] Vernerey *et al.*[150–152] should be mentioned here.

4. Discontinuous Computational Homogenization Models

Discontinuous CH models are developed to define the behavior of discontinuities (usually cracks) at macroscale from nested microscopic FE computations. This section describes two CH schemes for multiscale modeling of adhesive and cohesive cracks.

Homogenization towards intrinsic cohesive laws[a] that govern the behavior of heterogeneous material layers has been presented in Matouš *et al.*,[92] Kulkarni *et al.*[72] where microscale failure is modeled by a continuum damage model. A multiscale approach to capture the behavior of material layers that possess a micromorphic mesostructure is presented in Hirschberger *et al.*[48] Alfaro *et al.*[2] presented a similar work in which discrete cohesive cracks are adopted to represent microscopic failure. Computational homogenization schemes (in the context of an FE^2 method) for heterogeneous material layers has been given in Hirschberger *et al.*[49] for finite deformation problems, Kulkarni *et al.*,[73] Verhoosel *et al.*,[149] Nguyen *et al.*[109] for small strain problems.

Homogenization towards extrinsic cohesive laws[b] that govern the behavior of cohesive cracks was presented for the first time in Verhoosel *et al.*[148,149] for random heterogeneous materials exhibiting discrete cracking and later in Nguyen *et al.*[109] for random heterogeneous materials displaying a localization band.

4.1. *Homogenization towards an initially elastic cohesive law*

Let us consider a solid with a heterogeneous material layer, see Fig. 8. The thickness of the layer is denoted by t_{adh}. At the macroscale, the finite thickness layer is modeled as a set of zero thickness interface elements (see e.g., Refs. 7 and 156). The constitutive behavior of these interface elements — the so-called initially elastic cohesive law is coming from microscale FE computations performed on a micro-sample with the height being t_{adh}, and in which the microstructure of the layer is fully resolved.

The general procedure of the scheme is given in Fig. 9(a). Boundary conditions applied on the RVE are shown in Fig. 9(b). It is emphasized that these BCs are defined intuitively based on the geometry interpretation of the problem. Periodic

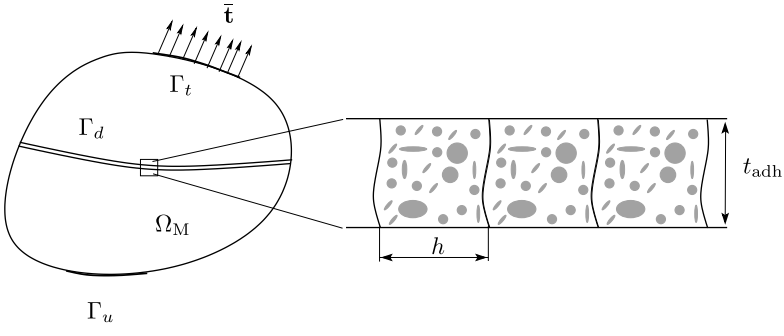

Fig. 8. A two-dimensional solid with a heterogeneous layer.

[a]Also known as initially elastic cohesive laws.
[b]Also known as initially rigid cohesive laws.

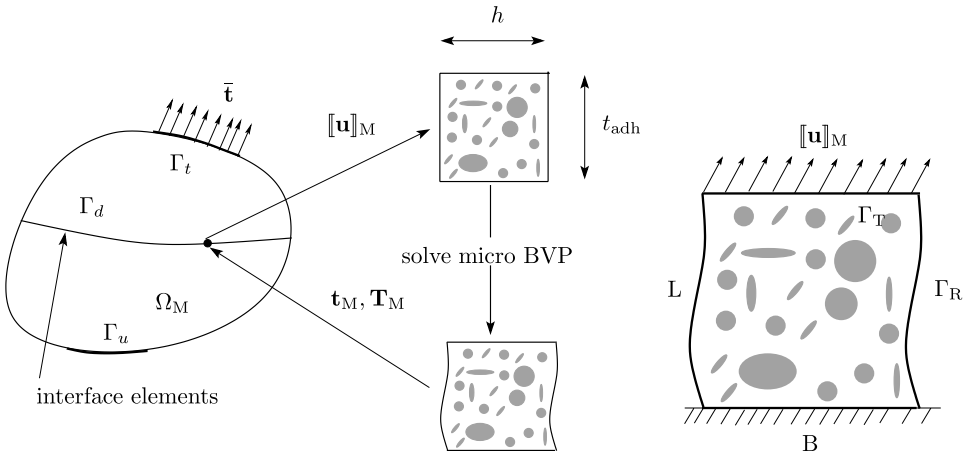

Fig. 9. Computational homogenization for material layers. Semi periodic BCs are imposed on the RVE: (a) FE^2 scheme for interface homogenization and (b) BCs for the RVE.

BCs on the left and right edges read $\mathbf{u}_{\mathrm{L}} = \mathbf{u}_{\mathrm{R}}$ and $\mathbf{t}_{\mathrm{R}} = -\mathbf{t}_{\mathrm{L}}$. This BC is referred to as an semi-periodic BC in Hirschberger *et al.*[49]

The micro-to-macro transition is also based on the Hill–Mandel principle that now reads

$$\mathbf{t}_{\mathrm{M}} \cdot \delta \llbracket \mathbf{u} \rrbracket_{\mathrm{M}} = \frac{1}{h} \int_{\Gamma_{\mathrm{m}}} \mathbf{t}_{\mathrm{m}} \cdot \delta \mathbf{u}_{\mathrm{m}} \mathrm{d}\Gamma_{\mathrm{m}} \tag{8}$$

where h denotes the width of the micro sample. Note that since the material layer is modeled as a line at the macroscale, homogenization of the material layer is one-dimensional homogenization along the direction parallel to the layer. The above equation can be rewritten as follows (see Fig. 9(b) for notations)

$$\begin{aligned} \mathbf{t}_{\mathrm{M}} \cdot \delta \llbracket \mathbf{u} \rrbracket_{\mathrm{M}} &= \frac{1}{h} \left[\left(\int_{\Gamma_{\mathrm{T}}} \mathbf{t}_{\mathrm{m}} \mathrm{d}\Gamma_{\mathrm{m}} \right) \cdot \delta \llbracket \mathbf{u} \rrbracket_{\mathrm{M}} + \int_{\Gamma_{\mathrm{R}}} \mathbf{t}_{\mathrm{m}} (\delta \mathbf{u}_{\mathrm{R}} - \delta \mathbf{u}_{\mathrm{L}}) \mathrm{d}\Gamma \right] \\ &= \frac{1}{h} \left(\int_{\Gamma_{\mathrm{T}}} \mathbf{t}_{\mathrm{m}} \mathrm{d}\Gamma_{\mathrm{m}} \right) \cdot \delta \llbracket \mathbf{u} \rrbracket_{\mathrm{M}} \end{aligned} \tag{9}$$

where periodic BCs of the displacements on the right and left edges together with anti-periodicity of the traction on these edges have been used. Since this equation holds for any $\delta \llbracket \mathbf{u} \rrbracket_{\mathrm{M}}$, one obtains

$$\mathbf{t}_{\mathrm{M}} = \frac{1}{h} \int_{\Gamma_{\mathrm{T}}} \mathbf{t}_{\mathrm{m}} \mathrm{d}\Gamma_{\mathrm{m}} \tag{10}$$

This line of derivation shares similarity with the one given in Ref. 2.

As shown in Refs. 2, 72 and 92, when h is sufficiently large (note that t_{adh} is kept fixed), the homogenized initially elastic cohesive law $(\mathbf{t}_{\mathrm{M}}, \llbracket \mathbf{u} \rrbracket_{\mathrm{M}})$ becomes

independent of h. In other words, an RVE exists for this kind of homogenization. Verhoosel *et al.*[149] presented a formulation wherein the height of the RVE can be smaller than the layer thickness t_{adh}.

4.2. *Homogenization towards an initially rigid cohesive law from a microscale crack*

The first discontinuous CH scheme for modeling cohesive failure in random heterogeneous solids, which is presented in Verhoosel *et al.*,[149] is given in Fig. 10. The macroscopic bulk is assumed to be linear elastic with effective properties computed *a priori* using the continuous CH model presented in Sec. 2. When the macroscopic stresses satisfy a failure criterion, a crack is inserted at the macroscale. The extrinsic cohesive law of the crack is computed from nested FE computations realized on micro samples attached to Gauss points on the crack. Microscale failure is represented by discrete cohesive cracks discretized using zero-thickness interface elements.

The Hill–Mandel theorem for the micro-to-macro transition reads[149]

$$\boldsymbol{\sigma}_{\text{M}} : \delta\boldsymbol{\epsilon}_{\text{M}} + \frac{1}{w}\mathbf{t}_{\text{M}} \cdot \delta[\![\mathbf{u}]\!]_{\text{M}} = \frac{1}{wh}\int_{\Gamma_{\text{m}}} \mathbf{t}_{\text{m}} \cdot \delta\mathbf{u}_{\text{m}} \text{d}\Gamma \tag{11}$$

We are going to prove that Eq. (11) is equivalent to the following Hill–Mandel equation which indicates that the behavior of the macro crack is coming from the micro cracks

$$\mathbf{t}_{\text{M}} \cdot \delta[\![\mathbf{u}]\!]_{\text{M}} = \frac{1}{h}\int_{\Gamma_{\text{m}}^{\text{c}}} \mathbf{t}_{\text{m}} \cdot \delta[\![\mathbf{u}]\!]_{\text{m}} \text{d}\Gamma \tag{12}$$

The proof is as follows. The microscale virtual work equation reads

$$\int_{\Omega_{\text{m}}} \boldsymbol{\sigma}_{\text{m}} : \delta\boldsymbol{\epsilon}_{\text{m}} \text{d}\Omega + \int_{\Gamma_{\text{m}}^{\text{c}}} \mathbf{t}_{\text{m}} \cdot \delta[\![\mathbf{u}]\!]_{\text{m}} \text{d}\Gamma = \int_{\Gamma_{\text{m}}} \mathbf{t}_{\text{m}} \cdot \delta\mathbf{u}_{\text{m}} \text{d}\Gamma \tag{13}$$

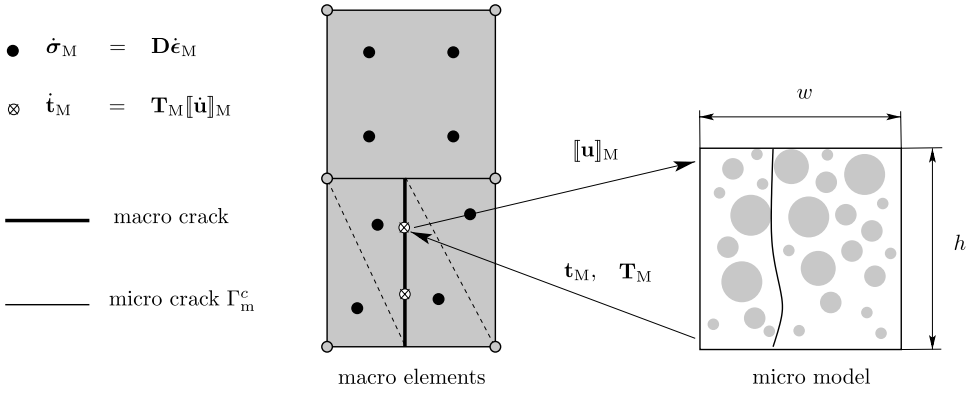

Fig. 10. Discontinuous CH scheme for cohesive crack modelling in heterogeneous solids[149] where microscopic failure is represented by discrete cracks. Black circles denote bulk GPs while crossed circles are cohesive GPs.

where the first term represents the internal work done by the bulk material and the second term expresses the internal work performed by the micro cracks and the third term denotes the external work.

The Hill–Mandel condition for the bulk reads

$$\boldsymbol{\sigma}_{\mathrm{M}} : \delta\boldsymbol{\epsilon}_{\mathrm{M}} = \frac{1}{wh} \int_{\Omega_{\mathrm{m}}} \boldsymbol{\sigma}_{\mathrm{m}} : \delta\boldsymbol{\epsilon}_{\mathrm{m}} \mathrm{d}\Omega \tag{14}$$

Substitution of Eqs. (12) and (14) into Eq. (13) yields Eq. (11). This concludes the proof.

It has been shown, in Ref. 149, that when there is a dominant crack running through the microscopic sample, the homogenized cohesive law is objective with respect to the size of the microscopic sample. Note that Eq. (12) ensures the objectivity of the homogenized cohesive law. The main features of this method are as follows

- Failure at macroscale and microscale are modeled using cohesive cracks. Macroscopic cracks are treated using the extended finite element method (XFEM), see e.g., Refs. 8, 28 and 154 while microscopic cracks are modeled using interface elements;
- Macroscopic bulk behaves linear elastically with effective properties;
- Initiation/propagation and orientation of macroscopic cracks are determined on the basis of the macro-stress field;
- The method allows for a definition of an RVE for softening materials exhibiting discrete failure.

4.3. *Homogenization towards an initially rigid cohesive law from a microscale localization band*

In Nguyen *et al.*[109,110] an extension of the multiscale cohesive crack CH model, presented in Sec. 4.2, was given. The major difference with the work of Verhoosel *et al.*[149] is that microscopic failure is modeled in a smeared fashion via a nonlocal continuum damage theory. The method is based on the *failure zone averaging scheme* proposed by Nguyen *et al.*[108] wherein the averaging is not performed over the entire RVE but over a propagating damaged domain. Figure 11 shows the transition from a microscopic localization band to a macroscopic crack and the scheme of the method is given in Fig. 12.

Let us first denote Ω_{d} as the active damaged domain i.e., the region containing Gauss points which are damaged and loading. For an isotropic continuum damage model, Ω_{d} is mathematically defined as

$$\Omega_{\mathrm{d}} = \{\mathbf{x} \in \Omega_{\mathrm{m}} \mid \omega(\mathbf{x}) > 0, f(\mathbf{x}) = 0\} \tag{15}$$

where ω is a scalar damage variable and f is the loading function.

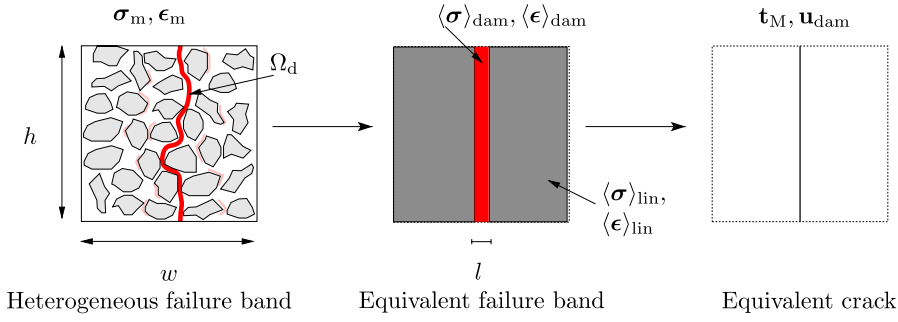

Fig. 11. From a microscale localization band to a macroscale equivalent crack via an energetic equivalence consideration.

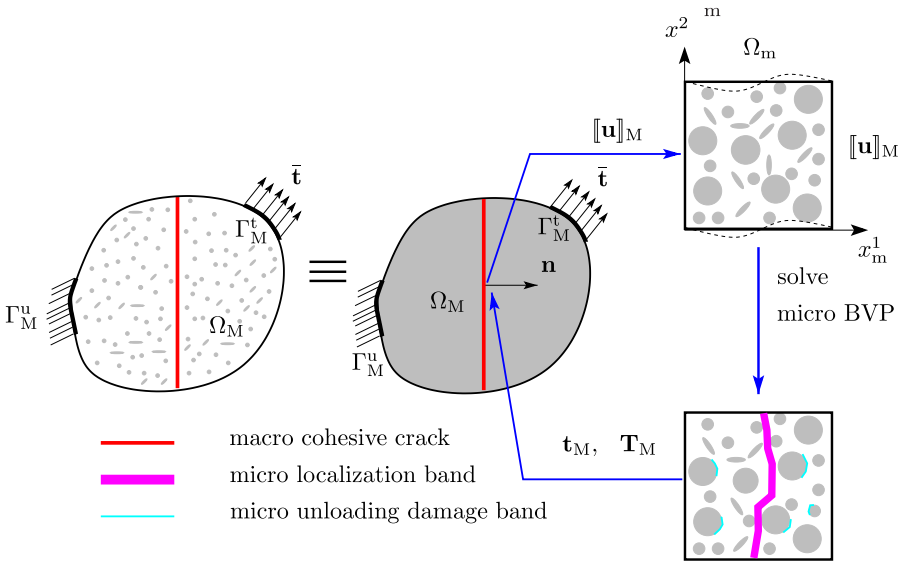

Fig. 12. Schematic representation of the multiscale cohesive crack scheme. Dotted lines represent periodic boundary conditions.

The micro-to-macro transition is based on the following equation

$$\frac{1}{wh}\int_{\Omega_{\mathrm{d}}} \boldsymbol{\sigma}_{\mathrm{m}} : \delta\boldsymbol{\epsilon}_{\mathrm{m}} \mathrm{d}\Omega = \frac{1}{w}\mathbf{t}_{\mathrm{M}} \cdot \delta\mathbf{u}_{\mathrm{dam}} \tag{16}$$

which states the equivalence of energy in the microscopic damaged domain and energy of the macroscopic crack. Note the similarity of this equation with Eq. (12). The final micro-macro linking is given by

$$\mathbf{u}_{\mathrm{R}} = (w-l)\mathbf{C}_0 \cdot \mathbf{t}_{\mathrm{M}} + [\![\mathbf{u}]\!]_{\mathrm{M}} + \mathring{\mathbf{u}}_{\mathrm{dam}} \tag{17}$$

where $\mathbf{u}_{\mathrm{R}}$ is the total displacement of the RVE, and $\mathring{\mathbf{u}}_{\mathrm{dam}}$ the compatibility displacement. In the above, $l = |\Omega_{\mathrm{d}}|/h$ defines the averaged width of the microscopic localization band, see Fig. 11. The matrix $\mathbf{C}_0$ is the projection of the compliance $\mathbf{D}_0^{-1}$ on the crack plane ($\mathbf{D}_0$ is $\mathbf{D}_{\mathrm{M}}$ evaluated in the undeformed RVE).

During the macroscale analysis, for a Newton–Raphson iteration when the traction for an GP on the crack (having a jump $[\![\mathbf{u}]\!]_{\mathrm{M}}$) is needed (the macro-bulk is assumed to be linear elastic, hence for bulk GPs there is no need to solve any RVE problems), the following system of equations is solved for $\mathbf{u}_{\mathrm{m}}$ and $\mathbf{t}_{\mathrm{M}}$

$$\mathbf{f}_{\mathrm{int}}(\mathbf{u}_{\mathrm{m}}) = \mathbf{f}_{\mathrm{ext}}([\![\mathbf{u}]\!]_{\mathrm{M}}) \tag{18}$$

$$\mathbf{u}_{\mathrm{R}}(\mathbf{u}_{\mathrm{m}}) = [w - l(\mathbf{u}_{\mathrm{m}})]\mathbf{C}_0\mathbf{t}_{\mathrm{M}} + [\![\mathbf{u}]\!]_{\mathrm{M}} + \mathring{\mathbf{u}}_{\mathrm{dam}} \tag{19}$$

which consists of the micro equilibrium equation and the homogenization relation Eq. (17). In the above, $\mathbf{f}_{\mathrm{int}}$ and $\mathbf{f}_{\mathrm{ext}}$ are the microscopic internal and external force vectors, respectively. This system of equations is solved iteratively in the sense that a guess value for $\mathbf{u}_{\mathrm{R}}$ is assumed, Eq. (18) is first solved (again iteratively using for instance the Newton–Raphson method) and then Eq. (19) is checked. This process is repeated until both equations are satisfied. The convergence of this process was studied in the paper of Nguyen *et al.*[110] Note that in most of FE^2 methods, at a certain Newton–Raphson iteration used to solve the macroscale problem, the microscale equilibrium equation (18) has to be solved only once. In the MAD method,[9,10] the microscopic equilibrium also has to be solved a couple of times due to the use of mixed BCs (see Sec. 5 for details).

The models proposed by Verhoosel *et al.*,[149] Nguyen *et al.*[109] assumed that the pre-failure nonlinear (hardening) part of the micro-model response, indicated in Fig. 13 by the darker region, is negligible. Therefore, the macroscopic bulk always behaves linear elastically and thus there is no need to solve any RVE problem to compute the macroscopic bulk stresses. This assumption dramatically reduces the cost of the method.

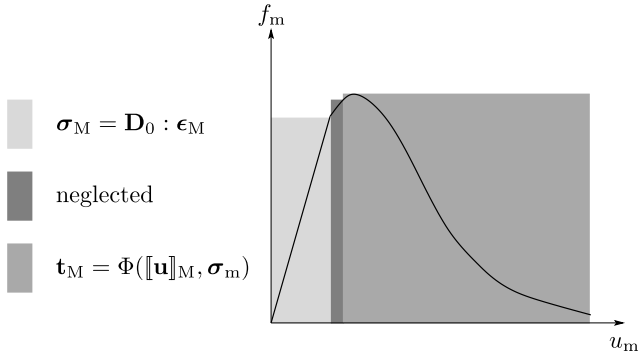

Fig. 13. Coupling between macro- and micro-models for cohesive crack modelling.

5. Continuous-Discontinuous Computational Homogenization Models

Continuous-discontinuous CH methods refer to CH models in which the macroscopic bulk and discontinuities are coupled to RVE computations. These models were developed to model the transition from micro-cracks to macro-cracks as usually observed in reality. Basically, when material instabilities (in form of cracks and/or shear bands) are detected at a certain RVE, a crack is injected at the macroscopic point linked to this RVE. This section gives an overview of existing methods falling within this category.

5.1. *Work of Massart et al.*

Probably the first CH model that works for strain localization problems was the work of Massart *et al.*[90,91] in the context of masonry cracking. To regularize the macroscopic continuum, a strain discontinuity with a given width is introduced at the integration point to which the associated RVE shows localization. The strain discontinuity was, however, not explicitly incorporated in the coarse scale discretization as such, but was rather embedded in the averaged behavior of the considered quadrature point. Characteristics of the method are (see Fig. 14):

- Microscopic failure is modeled via a nonlocal continuum damage model;
- Macroscopic localization is represented by a strain discontinuity of finite width that is defined from the periodicity of the considered masonry material;
- The onset of macroscopic localization is based on the loss of positive definiteness of the homogenized material tangent matrix $\mathbf{D}_{\mathrm{M}}$;
- The orientation of the macroscopic localization band is the averaged orientation of the microscopic localization band that is determined using the acoustic tensor associated to $\mathbf{D}_{\mathrm{M}}$.

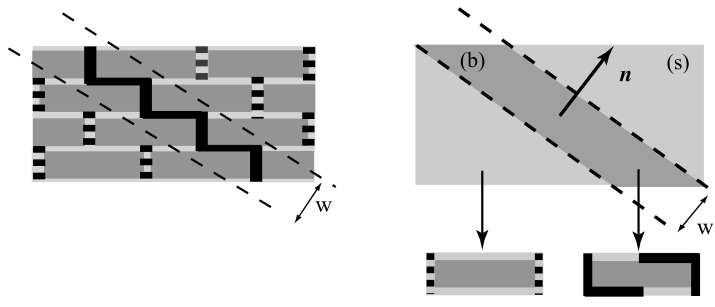

Fig. 14. Enhanced CH model for masonry failure-idealization of the constitutive response of a macroscopic integration point: localization band width w associated to the microscopic failure pattern (left) and two RVEs wherein one is associated to the band and one is associated to the unloading surrounding volume (right). The thick black line denotes the localization band and the dashed line represents unlocalized damage. Adapted from Massart *et al.*[91]

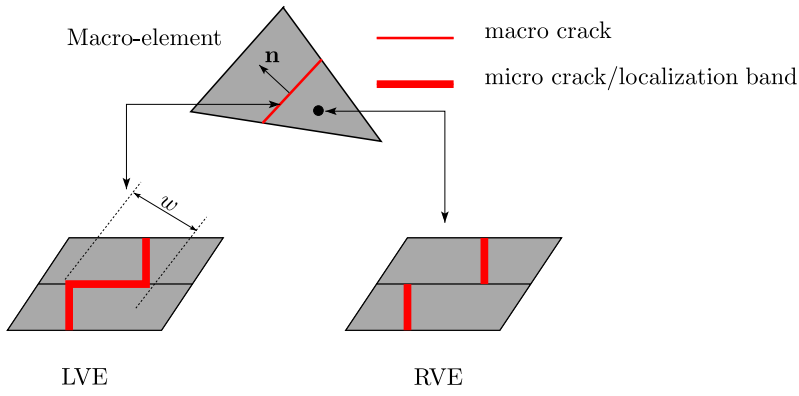

Fig. 15. Schema of the continuous-discontinuous CH scheme for masonry developed by Mercatoris and Massart.[94] LVE stands for localizing volume element which is coupled to the macro-crack. Note that damage is frozen in the RVE associated to the bulk of a cracked element.

Recently, the scheme in Massart *et al.*[90] has been extended by Mercatoris and Massart[94] in which macroscopic localization is modeled with cohesive cracks, see Fig. 15. The macroscopic discrete cracks are discretized using the embedded discontinuity approach, see e.g., Ref. 85. The continuity of crack path across the element boundary was not enforced. This work derived a macroscopic cohesive law from a damaging RVE for masonry materials. Note that the macro-crack can rotate subsequently after being inserted.

For a macro-element with a crack having a normal denoted by $\mathbf{n}$ and an opening represented by $[\![\mathbf{u}]\!]_{\mathrm{M}}$, the strain field to be imposed on the localizing volume element (LVE) is given by

$$\boldsymbol{\epsilon}^{\mathrm{LVE}} = \frac{1}{2w}\left([\![\mathbf{u}]\!]_{\mathrm{M}}\mathbf{n} + \mathbf{n}[\![\mathbf{u}]\!]_{\mathrm{M}}\right) \tag{20}$$

Note that in their implementation, the crack jump inside one macro-element is constant. Therefore, there is only one LVE associated to one cracked macro-element. The strain corresponding to the crack $\boldsymbol{\epsilon}^{\mathrm{LVE}}$ is then imposed on the boundary of the RVE using periodic BCs. After solving the RVE problem, the macro traction is computed as

$$\mathbf{t}_{\mathrm{M}} = \mathbf{n} \cdot \boldsymbol{\sigma}^{\mathrm{LVE}} \tag{21}$$

5.2. *Work of Belytschko et al.*

In Belytschko *et al.*,[10] Belytschko and Song[9] the MAD method was presented of which the essential feature is the injection of an equivalent crack at the macroscopic model when material instabilities (such as cracks or shear bands) occur at the microscopic sample. Both micro and macro cracks are solved by the XFEM approach. Compared to other CH based multiscale failure models, a substantial difference is that the fine scale analysis determines an equivalent traction-free crack

(not a cohesive crack) to be injected at macroscale. In other words, unit cell computations provide both the opening and orientation for the equivalent crack. The nodal positions of macro-elements are adjusted to take this crack opening into account. The bulk stress is the standard volume average of the microscopic stress. No homogenized tangent moduli are needed since the macroscopic BVP is solved using the dynamic relaxation method with an explicit time integrator. More applications of the MAD method were given in Song and Belytschko.[132] Characteristics of the MAD method are:

(1) Averaging operations are performed on the so-called *perforated unit cells* which are unit cells that excludes cracks and localization bands;
(2) Continuous evolving cracks can be modeled at the coarse scale;
(3) An equivalent macro crack can rotate in time after being introduced in the macro element;
(4) Utilization of hourglass modes to better capture the deformed shape for a rectangular unit cell with a growing crack.

In order to treat the hourglass modes, two generalized hourglass strains and two corresponding generalized stresses are added to the kinematic and kinetic description at macroscale. These generalized stresses are defined by using a generalized Hill–Mandel principle in the same spirit as in Kouznetsova *et al.*[69]

As boundary conditions are concerned, the MAD method employs two kinds of BCs namely linear BCs for unit cells without cracks near to the unit cell boundary and a combination of linear BCs and constant traction BCs for unit cells with a crack going to reach the boundary. A constant traction BC is used for the portion of the boundary in the neighborhood of a crack whereas a linear BC is adopted for the remaining boundary. Note that the linear BCs are enriched with hourglass modes.

However the current version of the MAD method has the following limitations

- The unit cell exactly matches the macroscopic element to which it is linked. In this regard, the MAD method shares the same idea with the coupled-volume method proposed by Ref. 37;
- Since RVEs are usually rectangles in two dimensions, the macroscopic domain must be discretized by four-noded quadrilateral elements (with one point quadrature rule);
- An explicit time integration scheme was used to solve the static equilibrium problem at macroscale. This choice was needed to avoid the snapback behavior on the equilibrium paths according to the authors. Therefore, an expression for the homogenized material tangent (required if a Newton–Raphson method is used) has not been provided.

Although the method is able, in principle, to compute an equivalent crack injected at macroscale from a field of micro-cracks, numerical examples involving

two scales deal only with one crack at microscale. This is due to the fact that, at microscale, a simple unit cell was used (matrix reinforced by one fiber).

5.3. *Work of Allen et al.*

Allen and his co-workers have developed homogenization-based multiscale frameworks for impact modeling of heterogeneous viscoelastic materials containing a field of evolving micro-cracks.[133,134] Crack propagation at microscale is modeled by a micromechanically derived cohesive law[c] presented in Allen and Searcy.[3] Adaptive insertion of zero-thickness interface elements was used to get a computationally efficient scheme for modeling cohesive micro-cracks. In Ref. 133, inertial effects were considered for the case of a statistically homogeneous field of micro-cracks i.e., micro-cracks do not form a localization band and hence no crack is injected at macroscale. Souza and Allen[134] extended their model to allow localization of micro-cracks into a macro-crack. However the formulation in Souza and Allen[134] is restricted to quasi-static conditions.

The method is summarized in Fig. 16. The characteristics of the method are as follows

- The initiation of macro-cracks is based on a modified version of the loss of ellipticity condition

$$\det[Q^0_{ij}(t)] \leq X_c \det[Q^0_{ij}(t=0)] \tag{22}$$

  where X_c is a critical percentage number, considered as a material constant and $Q^0_{ij}(t)$ is the acoustic tensor defined in terms of the homogenized material tangent;
- The orientation of a macro-crack is determined by minimizing $\det[Q^0_{ij}(t)]$;
- Once inserted, the macro-crack is not allowed to change its orientation;

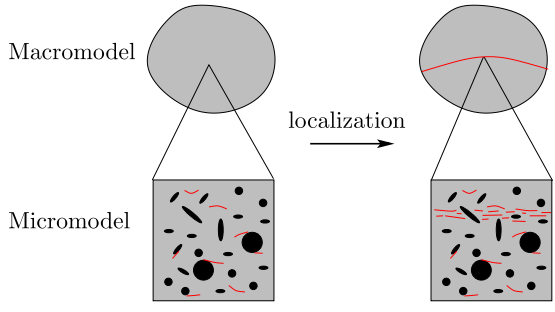

Fig. 16. Schematic representation of the multiscale scheme of Souza and Allen.[134] Short red lines denote evolving micro-cracks and the long red line represents the equivalent macro-crack (color online).

[c]This cohesive law is derived taking into account the structure of the material at one length scale lower. Therefore, in their work, three length scales are involved.

- For cracked macro-elements, cohesive micro-cracks are not allowed to propagate in RVEs associated to the bulk integration points;
- Constant strain triangular elements are used to discretize the macroscopic solid.

The last point deserves further explanation. As the XFEM method is used to model macro-cracks, once a crack is inserted, new GPs are created including bulk GPs locating on both sides of the crack and cohesive GPs on the crack surface, see Fig. 17. Constant strain triangular elements are used since they need only one GP for numerical integration purposes. The RVEs assigned to the newly created GPs are simply copies of the original RVE (at the moment of macro-crack initiation).

5.4. *Work of Nguyen et al.*

As mentioned previously, the discontinuous CH scheme for cohesive failure modelling presented in Refs. 109 and 110 assumes a linear elastic behavior of the macroscopic bulk. Recently, Nguyen *et al.*,[112] Nguyen[107] extended this CH scheme to a continuous-discontinuous CH framework wherein the macroscopic bulk is also coupled to RVEs. Figure 18 gives a sketch of the scheme.

The main features of this method are listed as follows

- Applied to random heterogeneous materials;
- The initiation of macro-cracks is based on the loss of positive definiteness of the homogenized material tangent matrix $\mathbf{D}_{\mathrm{M}}$;

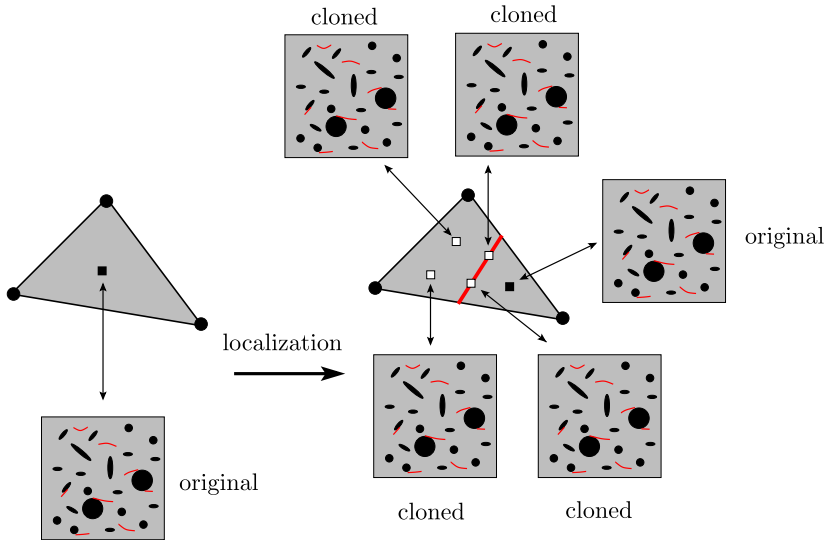

Fig. 17. RVE cloning in a constant strain element: once a crack is inserted in the macro-element, four new integration points are created. The RVEs for these points are simply cloned from the original RVE. Short red lines denote evolving micro-cracks.

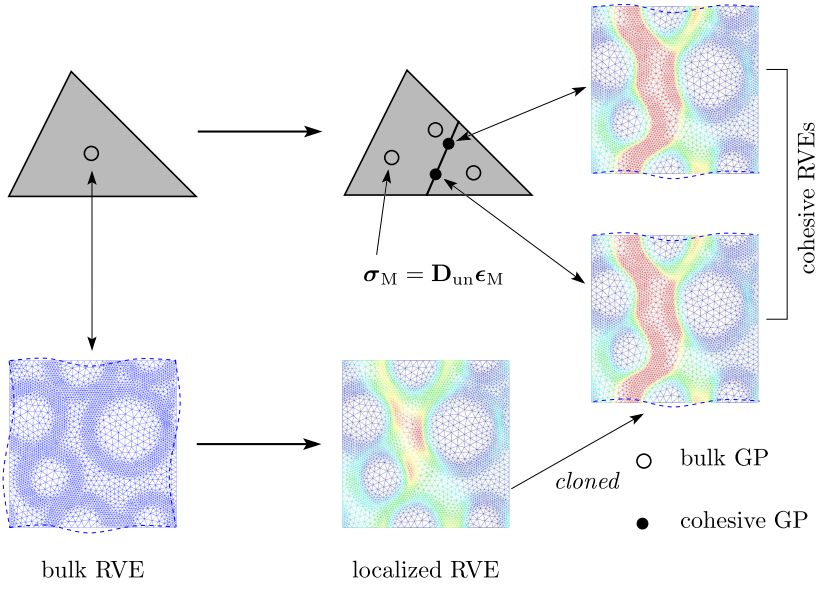

Fig. 18. The fully multiscale homogenization scheme. Initially bulk GPs are coupled with RVEs. When localization occurs in one of the RVEs, a macro-crack is inserted at the corresponding macro-element. Henceforth, cohesive GPs are coupled to RVEs that are *cloned* from the localized RVE. The bulk GPs of the cracked macro-element follow a secant unloading path. Dotted lines denote periodic boundary conditions.

- The orientation of the macro-cracks is determined using a criterion based on the macro-stress field;
- Allows a definition of an RVE for softening materials exhibiting localized deformation;
- Macroscopic domain can be discretized by any type of continuum element such as three-noded triangular or four-noded quadrilateral elements;
- An evolutionary BC for localized RVEs.

The final point deserves elaboration. At the start of the analysis, periodic BCs are imposed on the bulk RVE. When localization occurs at this RVE, a macro-crack is injected at the macro-element associated to this bulk RVE. The cohesive RVEs attached to GPs on the crack are now subjecting to semi-periodic BCs, see Fig. 18.

A summary of continuous-discontinuous CH models available in the literature is given in Table 2. Note that since the models of Massart *et al.*,[90] Mercatoris and Massart[94] and Belytschko *et al.*,[10] Belytschko and Song[9] were applied to materials having a well defined unit cell, therefore their methods allow for a definition of an RVE. It has not been shown whether the model of Souza and Allen[134] is objective with respect to the size of the RVE. The method of Nguyen *et al.*[112] is objective with respect to the RVE size since it is based on the failure zone averaging technique.

Table 2. Overview of available continuous-discontinuous CH models for multiscale failure modelling of materials.

Name	Material	Macroscopic failure	Microscopic failure	Ma. elem.	RVE
Massart *et al.*	Masonry	Embedded band/cracks	Localization band	T3	Yes
Allen *et al.*	Random viscoelastic	Cohesive cracks	Field of cohesive cracks	T3	?
Belytschko *et al.*	Composite	Traction-free cracks	One cohesive crack	Q4	Yes
Nguyen *et al.*	Random heterogeneous	Cohesive cracks	Diffuse localization band	Any	Yes

One common feature of the methods of Mercatoris and Massart,[94] Souza and Allen,[134] Nguyen *et al.*[112] is the use of two RVEs — one for the bulk material homogenization and one for the crack homogenization. In the MAD method of Belytschko *et al.*,[10] Belytschko and Song[9] there is only one unit cell associated to a macro-element. However, the use of a perforated unit cell to provide stresses for the macroscopic bulk and the fact that deformation of micro-cracks defines the orientation and magnitude of the equivalent macro-crack make the MAD approach equivalent to the other methods in Table 2.

6. Computational Aspects

6.1. *Discretization methods for macro and micro problems*

In principle any numerical method can be adopted at macro and micro scales. In practice, FEM is the dominant method. At microscale, due to the complex microstructures, making a compatible FE mesh is often a tedious task. For this reason, specific FEM methods have been used to solve the microscale problems such as the Voronoi Cell Finite Element Method (VCFEM) developed by Ghosh and his co-workers, see Ghosh *et al.*[32] and a recent monograph,[31] and the XFEM approach, see e.g., Refs. 47, 63 and 82 wherein the structured FE meshes are independent of the microstructures. In a multiscale simulation of plant tissue deformation by Ghysels *et al.*,[34] while the macroscopic domain is discretized using FEM, at microscale, a mass-spring model is employed to describe the geometrical structure and basic properties of individual plant cells. The computation of the macroscopic stress tensor is based on the definition of virial stress, as defined in molecular dynamics.

Sfantos and Aliabadi[129] presented a multiscale boundary element method (BEM) for modeling material failure. The method can be considered as an BE^2 method since the BEM is adopted at both scales. This BE^2 method was applied to model the intergranular failure of polycrystalline brittle materials. The efficient BE discretization at microscale allows the utilization of different RVEs for different macroscopic points. Note that most of FE^2 simulations assumed a single RVE for

every macroscopic points. Macroscopic failure is modeled using a nonlocal integral continuum damage model that requires a characteristic length parameter l. However a discussion on the relation between l and the RVE size was not provided. Periodic BCs defined from a nonlocal strain field are imposed on the RVEs.

In the continuous-discontinuous CH model of Souza and Allen[134] in which the XFEM approach is used to discretize the macroscopic solid, the issue of cloning RVEs associated with old integration points to new integration points upon crack initiation was avoided by employing constant strain elements. In contrast to the XFEM, embedded discontinuities approaches utilize a standard numerical integration scheme before and after crack initiation. For this reason, embedded discontinuities approaches are superior than the XFEM methods in a continuous-discontinuous CH framework.

6.2. *Boundary conditions*

Implementation of linear BCs is straightforward and hence requires no further discussion. Usually, periodic and minimal kinematic BCs are treated as non-homogeneous multifreedom (or multipoint) constraints which can be enforced using either a penalty method, the Lagrange multipliers method or the master-slave method.[20] Miehe and Koch[99] presented a general implementation using Lagrange multipliers for periodic and constant traction BCs. In Ref. 58, a unified treatment of commonly used BCs (linear, periodic and constant traction) was given following the work of Ainsworth.[1] The aforementioned treatment of periodic BCs is referred to as a strong format according to Larsson *et al.*[78] This strong format of periodicity requires periodic FE meshes that cannot be obtained for non-periodic RVEs or when adaptive computations are about to be done on unstructured RVE meshes. A weak format of periodic BCs has been proposed in Larsson *et al.*[78] by which a periodic RVE mesh is no longer required. The FE formulation employs a mixed format in the sense that the discretization of the displacement field inside the RVE and the tractions on the boundary of the RVE are chosen independently.

Another treatment of periodic BCs applied to RVEs made of fiber composite materials can be found in Tyrus *et al.*[143] The method is simple and efficient. The RVE mesh is not required to be periodic and furthermore triangular RVEs can be handled. However the microstructure distribution must be periodic.

Boundary effects refer to cases wherein a single kind of boundary conditions is applied to every RVE regardless the fact whether the RVEs are coupled to the macroscopic boundary elements or to the interior elements, see Fig. 19. This issue has been noted by Refs. 10 and 22. If AB is a free edge then edge 14 should be free as well. An example taken from Nguyen *et al.*,[110] which is shown in Fig. 20, illustrates this boundary effect.

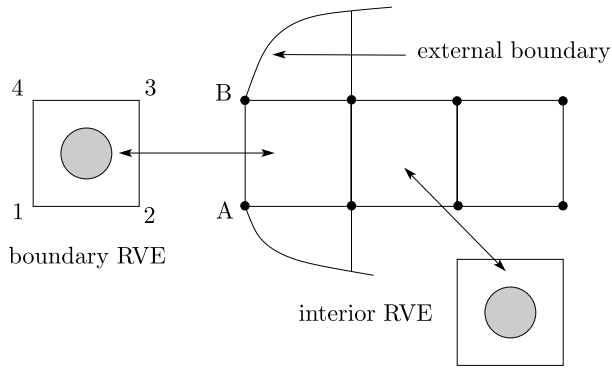

Fig. 19. The same BCs imposed on boundary RVEs and interior RVEs are not consistent with the free edge AB.

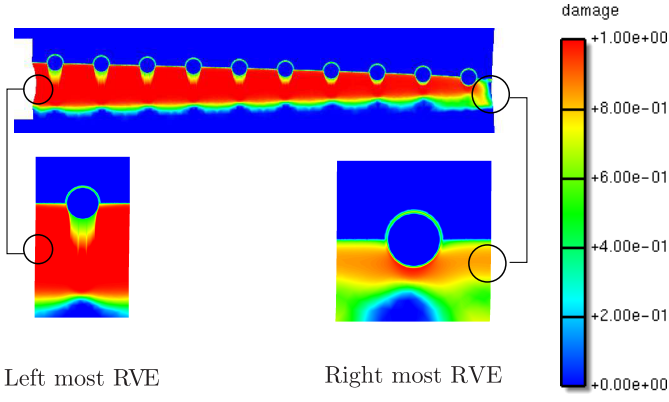

Fig. 20. Boundary effects in the discontinuous CH method: periodic boundary conditions are not suitable for boundary RVEs. The top figure shows the damage pattern in a direct numerical simulation. The bottom figure shows the damaging boundary RVEs.

6.3. *Reducing the computational cost*

CH models are naturally suitable for parallel computations since RVE computations are independent of each other. Each RVE is assigned to one processor and the RVE computations are performed in parallel, see e.g., Refs. 9, 10 and 23. The macroscopic computation is handled by a root (or master) processor in a sequential manner. Recently Nguyen *et al.*[111] presented a parallel implementation of the discontinuous CH method for modeling cohesive crack (see Sec. 4.3). According to Rahul and De,[125] the parallelization of multiscale CH models by using one root processor for the macroscopic domain and multiple slave processors for the RVEs is a naive and not efficient approach. To overcome this problem, they developed a novel coarse-grained parallel algorithm wherein groups of macroscale GPs are distributed to a layer of processors. Each processor in this layer communicates locally

with a group of processors that are responsible for the microscale computations. The overlapping groups of processors are shown to achieve optimal concurrency at signficantly reduced communication overhead. The conclusion made by Rahul and De[125] was, however, based on an explicit FE formulation employed at macroscale.

Another option for improving the speed of CH-based simulations can be based on a selective usage of CH models. In non-critical regions, a phenomenological or a micromechanically derived constitutive model is adopted whereas a CH model is realized for hot spots.[33,163] The partition of the macro solid into non-critical domains and hot spots is usually realized adaptively based on error analysis in quantities of interest. In the context of multiscale modeling of heterogeneous adhesive layers, Kulkarni *et al.*[73] also performed an adaptive homogenization scheme. A coupled microscopic analysis is performed only for Gauss points of the macroscopic cohesive elements that are in the region near a crack tip, whereas a precomputed linear constitutive law is used at Gauss points away from the active region.

Model reduction techniques provide an efficient tool to dramatically reduce the computational expense of CH simulations. The first work that uses model reduction methods in a CH context is done by Yvonnet and He.[160] The authors proposed a method coined R3M which stands for Reduced Model Multiscale Method. In a recent work, the R3M was used to solve highly nonlinear conduction problems in structures made of periodic heterogeneous materials.[102] The main characteristics of the R3M are as follows

- Continuous first-order FE^2 framework for finite strain hyperelasticity problems;
- A reduced order model (ROM) using a proper orthogonal decomposition (POD) is applied to the microscopic models. In other words, the equations of the linearized micro problem are projected on a fixed reduced basis;
- The reduced basis is computed on the basis of a number of so-called snapshots. Snapshots are determined from pre-computations on the RVEs.

Reduced order models have been developed so far mainly for problems without damage and/or strain localization. The main challenge for damage and failure problems is that a single reduced basis, which is computed *a priori*, is not sufficient for representing the behavior of materials having an evolving morphology. First attempts on extending ROMs to strain localization problems have recently appeared, see Refs. 65 and 66. Recently, Lamari *et al.*[74] used proper generalized decomposition (PGD) to reduce the cost of computational homogenization models. We refer to Néron and Ladevèze[105] and references therein for a thorough presentation of the PGD method for multiscale and multiphysics problems. It is our belief that POD/PGD when used in a continuous-discontinuous CH scheme would tremendously reduce the computational cost of multiscale simulations of material failure.

Oskay and Fish,[116] Yuan and Fish[158] presented a novel model reduction approach for periodic heterogeneous solids, which combines the asymptotic

expansion method with the transformation field analysis (TFA) to reduce the computational cost of a CH approach.

Finally, the artificial neural network discussed in Sec. 3 can be used to compute effective cohesive laws from a large number of detailed micromechanical analyses. This will enable large scale simulations of failure of structures.

6.4. *Robustness issues*

The robustness of FE^2 simulations depend on the robustness of the nested microscopic FE models. If one microscopic FE model fails to converge, the stresses at the corresponding macroscopic integration point cannot be found and the multiscale simulation crashes. There are basically two cases wherein the divergence of the microscopic FE problems occurs. In the first case, the macroscopic kinematic variable transferred to the RVE boundary is too large and thus the microscopic problem cannot be resolved in one single step. Somer *et al.*[131] proposed a substepping scheme to solve this problem. In the second case, snapback is happening at microscale. To the best of the authors' knowledge, a treatment of microscopic snapback in a FE^2 analysis has not appeared yet.

Handling macroscopic snapback in a multiscale analysis has been presented in Massart *et al.*,[89] Nguyen *et al.*[110] In Ref. 110, the simple yet efficient energy-based arc-length control developed by Gutiérrez,[41] Verhoosel *et al.*[147] was used.

Nezamabadi *et al.*[106] presented a combination of the FE^2 method and the asymptotic numerical method[12] for modeling the geometrical instabilities of heterogeneous materials. The asymptotic numerical method allows for the treatment of instabilities at both macro and micro scales without resorting to path following (also known as arc-length) methods.

7. Dynamics Problems

Most of the multiscale CH models developed so far in literature neglect inertial effects and are therefore not suitable for modeling heterogeneous materials subjected to dynamics loadings. Souza *et al.*[135] presented an FE^2 model for heterogeneous viscoelastic materials which is probably one of the first multiscale models that accounts for inertial effects. The most important assumption in this model is that the length of the wave propagating on the macroscale is much larger than the size of the microscopic length scale. Therefore, the microscopic initial boundary value problem (IBVP) can be simplified to a quasi-static equilibrium equation. The macroscopic IBVP is solved by an explicit FEM while the microscopic BVP is obtained by means of an implicit quasi-static FEM procedure. A two-dimensional multiscale method for impact modeling of viscoelastic solids having a random microstructure that contains a field of evolving micro-cracks has been given in Souza and Allen.[133] Although cracks are allowed at microscale, at macroscale, continuous deformation is assumed. Recently, Wiechert and Wall[155] presented a similar method which was applied in the context of bioengineering problems. The

novelty of this work is that a three dimensional formulation is considered for both length scales. Yet another feature is the utilization of the generalized-α time integration scheme for both scales.

8. Concluding Remarks and Challenges

We have reviewed relevant works in the field of multiscale modeling of heterogeneous materials. The emphasis was put on computational homogenization methods and strain localization/failure problems. It has been shown that a couple of schemes have been proposed to link microscopic localization to macroscopic failure. The developed multiscale methods were applied to masonry materials, fiber reinforced composite and random heterogeneous materials. Most of them are for quasi-brittle fracture.

Although large steps have been taken, there are still a number of unresolved issues that should be tackled in the years to come

- Dynamic problems;
- Boundary conditions and boundary effects;
- Robustness and efficiency issues;
- Uncertainty quantification;
- Continuous-discontinuous homogenization methods for ductile fracture;
- Model order reduction for strain localization problems at microscale;
- Validation of multiscale models against experimental results at multiple scales.

The final point deserves further discussion. The validation of a multiscale method poses some unique challenges. Validation of multiscale models is achieved when the discrepancy between experimental observations (of a quantity of interest) and the predictions of a calibrated multiscale model is small enough. Calibration of multiscale models is a difficult task since material constants used in multiscale models are defined at fine scales, often orders of magnitude smaller than the coarse scale at which experiments are conducted. Note that advancement in experimentation technologies can help to measure properties of the microstructural heterogeneities. In this sense Oskay and Fish[115] presented a calibration scheme for a particular multiscale model, the eigendeformation-based multiscale model.

Acknowledgments

The financial support from the Delft Center for Computational Science and Engineering (DCSE) is gratefully acknowledged.

References

1. M. Ainsworth, Essential boundary conditions and multi-point constraints in finite element analysis, *Comp. Methods Appl. Mech. Eng.* **190** (2001) 6323–6339.

2. M. V. Cid Alfaro, A. S. J. Suiker, C. V. Verhoosel and R. de Borst, Numerical homogenization of cracking processes in thin fibre-epoxy layers, *Eur. J. Mech. A/Solids* **29** (2010) 119–131.
3. D. H. Allen and C. R. Searcy, A micromechanical model for a viscoelastic cohesive zone, *Int. J. Fract.* **107** (2001) 159–176.
4. J. E. Andrade and X. Tu, Multiscale framework for behavior prediction in granular media, *Mech. Mater.* **41** (2009) 652–669.
5. J. E. Andrade, C. F. Avila, S. A. Hall, N. Lenoir and G. Viggiani, Multiscale modeling and characterization of granular matter: From grain kinematics to continuum mechanics, *J. Mech. Phys. Solids* **59** (2011) 237–250.
6. Z. P. Bažant, Can multiscale-multiphysics methods predict softening damage and structural failure? *Int. J. Multi. Comput. Eng.* **8** (2010) 61–67.
7. G. Beer, An isoparametric joint/interface element for finite element analysis, *Int. J. Numer. Meth. Eng.* **21** (1985) 585–600.
8. T. Belytschko and T. Black, Elastic crack growth in finite elements with minimal remeshing, *Int. J. Numer. Meth. Eng.* **45** (1999) 601–620.
9. T. Belytschko and J. H. Song, Coarse-graining of multiscale crack propagation, *Int. J. Numer. Meth. Eng.* **81** (2010) 537–563.
10. T. Belytschko, S. Loehnert and J. H. Song, Multiscale aggregating discontinuities: A method for circumventing loss of material stability, *Int. J. Numer. Meth. Eng.* **73** (2008) 869–894.
11. T. Christman, A. Needleman and S. Suresh, An experimental and numerical study of deformation in metal-ceramic composites, *Acta Metallurgica* **37** (1989) 3029–3050.
12. B. Cochelin, A path-following technique via an asymptotic-numerical method, *Comput. Struct.* **53** (1994) 1181–1192.
13. E. W. C. Coenen, V. G. Kouznetsova and M. G. D. Geers, Computational homogenization for heterogeneous thin sheets, *Int. J. Numer. Meth. Eng.* **83** (2010) 1180–1205.
14. W. A. Curtin and R. E. Miller, Atomistic/continuum coupling in computational materials science, *Model. Simul. Mater. Sci. Eng.* **11** (2003) R33–R68.
15. C. Dascalu, G. Bilbie and E. K. Agiasofitou, Damage and size effects in elastic solids: A homogenization approach, *Int. J. Solids Struct.* **45** (2008) 409–430.
16. E. A. de Souza Neto and R. A. Feijóo, On the equivalence between spatial and material volume averaging of stress in large strain multi-scale solid constitutive models, *Mech. Mater.* **40** (2008) 803–811.
17. H. B. Dhia and G. Rateau, The Arlequin method as a flexible engineering design tool, *Int. J. Numer. Meth. Eng.* **62** (2005) 1442–1462.
18. W. J. Drugan and J. R. Willis, A micromechanics-based nonlocal constitutive equation and estimates of representative volume element size for elastic composites, *J. Mech. Phys. Solids* **44** (1996) 497–524.
19. S. Eckardt and C. Könke, Adaptive damage simulation of concrete using heterogeneous multiscale models, *J. Algorithms Comput. Tech.* **2** (2008) 275–297.
20. C. A. Felippa, Introduction to Finite Element Methods, Multifreedom constraints I (lecture notes). (2001), http://www.colorado.edu/engineering/CAS/courses.d/IFEM.d/.
21. F. Feyel, Multiscale FE^2 elastoviscoplastic analysis of composite structures, *Comput. Mater. Sci.* **16** (1999) 344–354.

22. F. Feyel, A multilevel finite element method (FE^2) to describe the response of highly non-linear structures using generalized continua, *Comput. Meth. Appl. Mech. Eng.* **192** (2003) 3233–3244.
23. F. Feyel and J. L. Chaboche, FE^2 multiscale approach for modelling the elastoviscoplastic behaviour of long fibre SiC/Ti composite materials, *Comput. Meth. Appl. Mech. Eng.* **183** (2000) 309–330.
24. J. Fish, The s-version of the finite element method, *Comput. Struct.* **43** (1992) 539–547.
25. J. Fish, *Multiscale Methods: Bridging the Scales in Science and Engineering* (Oxford University Press, USA, 2009), ISBN 0199233853.
26. J. Fish, K. Shek, M. Pandheeradi and M. S. Shephard, Computational plasticity for composite structures based on mathematical homogenization: Theory and practice, *Comput. Meth. Appl. Mech. Eng.* **148** (1997) 53–73.
27. J. Fish, Q. Yu and K. Shek, Computational damage mechanics for composite materials based on mathematical homogenization, *Int. J. Numer. Meth. Eng.* **45** (1999) 1657–1679.
28. T. P. Fries and T. Belytschko, The extended/generalized finite element method: An overview of the method and its applications, *Int. J. Numer. Meth. Eng.* **84** (2010) 253–304.
29. M. G. D. Geers, V. G. Kouznetsova and W. A. M. Brekelmans, Multi-scale computational homogenization: Trends and challenges, *J. Comput. Appl. Math.* **234** (2010) 2175–2182.
30. J. Ghaboussi, J. Garret and X. Wu, Knowledge-based modeling of material behavior with neural networks, *J. Eng. Mech.* **117** (1991) 132–153.
31. S. Ghosh, *Micromechanical Analysis and Multi-Scale Modeling Using the Voronoi Cell Finite Element Method* (CRC Press, 2011).
32. S. Ghosh, K. Lee and S. Moorthy, Two scale analysis of heterogeneous elastic-plastic materials with asymptotic homogenization and Voronoi cell finite element model, *Comput. Meth. Appl. Mech. Eng.* **132** (1996) 63–116.
33. S. Ghosh, K. Lee and P. Raghavan, A multi-level computational model for multi-scale damage analysis in composite and porous materials, *Int. J. Solids Struct.* **38** (2001) 2335–2385.
34. P. Ghysels, G. Samaey, B. Tijskens, P. Van Liedekerke, H. Ramon and D. Roose, Multi-scale simulation of plant tissue deformation using a model for individual cell mechanics, *Phys. Biol.* **6** (2009) 016009.
35. I. M. Gitman, H. Askes and L. J. Sluys, Coupled-volume multi-scale modelling of quasi-brittle material, *Eur. J. Mech. A/Solids* **27** (2007a) 302–327.
36. I. M. Gitman, H. Askes and L. J. Sluys, Representative volume: Existence and size determination, *Eng. Fract. Mech.* **74** (2007b) 2518–2534.
37. I. M. Gitman, H. Askes and L. J. Sluys, Coupled-volume multi-scale modelling of quasi-brittle material, *Eur. J. Mech. A/Solids* **27** (2008) 302–327.
38. R. Grytz and G. Meschke, Consistent micro-macro transitions at large objective strains in curvilinear convective coordinates, *Int. J. Numer. Meth. Eng.* **73** (2008) 805–824.
39. J. M. Guedes and N. Kikuchi, Preprocessing and postprocessing for materials based on the homogenization method with adaptive finite element methods, *Comput. Meth. Appl. Mech. Eng.* **83** (1990) 143–198.
40. P. A. Guidault, O. Allix, L. Champaney and J. P. Navarro, A two-scale approach with homogenization for the computation of cracked structures, *Comput. Struct.* **85** (2007) 1360–1371.

41. M. A. Gutiérrez, Energy release control for numerical simulations of failure in quasi-brittle solids, *Commun. Numer. Meth. Eng.* **20** (2004) 19–29.
42. R. Hambli, Numerical procedure for multiscale bone adaptation prediction based on neural networks and finite element simulation, *Finite Elem. Anal. Des.* **47** (2011) 835–842.
43. S. Hazanov and C. Huet, Order relationships for boundary conditions effect in heterogeneous bodies smaller than the representative volume, *J. Mech. Phys. Solids* **42** (1994) 1995–2011.
44. T. Hettich, A. Hund and E. Ramm, Modeling of failure in composites by X-FEM and level sets within a multiscale framework, *Comput. Meth. Appl. Mech. Eng.* **197** (2008) 414–424.
45. R. Hill, Elastic properties of reinforced solids: Some theoretical principles, *J. Mech. Phys. Solids* **11** (1963) 357–372.
46. R. Hill, A self-consistent mechanics of composite materials, *J. Mech. Phys. Solids* **12** (1965) 213–222.
47. B. Hiriyur, H. Waisman and G. Deodatis, Uncertainty quantification in homogenization of heterogeneous microstructures modeled by XFEM, *Int. J. Numer. Meth. Eng.* **88** (2011) 257–278.
48. C. B. Hirschberger, N. Sukumar and P. Steinmann, Computational homogenization of material layers with micromorphic mesostructure, *Philos. Mag.* **88** (2008) 3603–3631.
49. C. B. Hirschberger, S. Ricker, P. Steinmann and N. Sukumar, Computational multiscale modelling of heterogeneous material layers, *Eng. Fract. Mech.* **76** (2009) 793–812.
50. M. Hori and S. Nemat-Nasser, On two micromechanics theories for determining micro-macro relations in heterogeneous solids, *Mech. Mater.* **31** (1999) 667–682.
51. C. Huet, Coupled size and boundary-condition effects in viscoelastic heterogeneous and composite bodies, *Mech. Mater.* **31** (1999) 787–829.
52. T. J. R. Hughes, G. R. Feijóo, L. Mazzei and J. B. Quincy, The variational multiscale method — a paradigm for computational mechanics, *Comput. Meth. Appl. Mech. Eng.* **166** (1998) 3–24.
53. C. Iacono, *Procedures for Parameter Estimates of Computational Models for Localized Failure*, Ph.D. thesis (Delft University of Technology, 2007).
54. A. Ibrahimbegović and D. Markovič, Strong coupling methods in multi-phase and multi-scale modeling of inelastic behavior of heterogeneous structures, *Comput. Meth. Appl. Mech. Eng.* **192** (2003) 3089–3107.
55. H. M. Inglis, P. H. Geubelle and K. Matouš, Boundary condition effects on multiscale analysis of damage localization, *Philos. Mag.* **88** (2008) 2373.
56. J. R. Jain and S. Ghosh, Damage evolution in composites with a homogenization-based continuum damage mechanics model, *Int. J. Damage Mech.* **18** (2009) 533–568.
57. J. W. Ju and H. K. Lee, A micromechanical damage model for effective elastoplastic behavior of ductile matrix composites considering evolutionary complete particle debonding, *Comput. Meth. Appl. Mech. Eng.* **183** (2000) 201–222.
58. L. Kaczmarczyk, C. J. Pearce and N. Bicanic, Scale transition and enforcement of RVE boundary conditions in second-order computational homogenization, *Int. J. Numer. Meth. Eng.* **74** (2008) 506–522.
59. L. Kaczmarczyk, C. J. Pearce and N. Bicanic, Studies of microstructural size effect and higher-order deformation in second-order computational homogenization, *Comput. Struct.* **88** (2010a) 1383–1390.

60. L. Kaczmarczyk, C. J. Pearce, N. Bicanic and E. de Souza Neto, Numerical multiscale solution strategy for fracturing heterogeneous materials, *Comput. Meth. Appl. Mech. Eng.* **199** (2010b) 1100–1113.
61. T. Kanit, S. Forest, I. Galliet, V. Mounoury and D. Jeulin, Determination of the size of the representative volume element for random composites: Statistical and numerical approach, *Int. J. Solids Struct.* **40** (2003) 3647–3679.
62. P. Kanouté, D. P. Boso, J. L. Chaboche and B. A. Schrefler, Multiscale methods for composites: A review, *Arch. Comput. Meth. Eng.* **16** (2009) 31–75.
63. M. Kästner, G. Haasemann and V. Ulbricht, Multiscale XFEM-modelling and simulation of the inelastic material behaviour of textile-reinforced polymers, *Int. J. Numer. Meth. Eng.* **86** (2011) 477–498.
64. M. Kawagai, A. Sando and N. Takano, Image-based multi-scale modelling strategy for complex and heterogeneous porous microstructures by mesh superposition method, *Model. Simul. Mater. Sci. Eng.* **14** (2006) 53–69.
65. P. Kerfriden, J. C. Passieux and S. P. A. Bordas, Local/global model order reduction strategy for the simulation of quasi-brittle fracture, *Int. J. Numer. Meth. Eng.* doi: 10.1002/nme.3234.
66. P. Kerfriden, P. Gosselet, S. Adhikari and S. Bordas, Bridging proper orthogonal decomposition methods and augmented Newton-Krylov algorithms: An adaptive model order reduction for highly nonlinear mechanical problems, *Comput. Meth. Appl. Mech. Eng.* **200** (2010) 850–866.
67. V. Kouznetsova, *Computational Homogenization for the Multi-Scale Analysis of Multi-Phase Materials*, Ph.D. thesis (Eindhoven University of Technology, 2002).
68. V. Kouznetsova, W. A. M. Brekelmans and F. P. T. Baaijens, An approach to micro-macro modeling of heterogeneous materials, *Comput. Mech.* **27** (2001) 37–48.
69. V. Kouznetsova, M. G. D. Geers and W. A. M. Brekelmans, Multi-scale constitutive modelling of heterogeneous materials with a gradient-enhanced computational homogenization scheme, *Int. J. Numer. Meth. Eng.* **54** (2002) 1235–1260.
70. V. G. Kouznetsova, M. G. D. Geers and W. A. M. Brekelmans, Multi-scale second-order computational homogenization of multi-phase materials: A nested finite element solution strategy, *Comput. Meth. Appl. Mech. Eng.* **193** (2004a) 5525–5550.
71. V. G. Kouznetsova, M. G. D. Geers and W. A. M. Brekelmans, Size of a representative volume element in a second-order computational homogenization framework, *Int. J. Multi. Comput. Eng.* **2** (2004b) 575–598.
72. M. G. Kulkarni, P. H. Geubelle and K. Matouš, Multi-scale modeling of heterogeneous adhesives: Effect of particle decohesion, *Mech. Mater.* **41** (2009) 573–583.
73. M. G. Kulkarni, K. Matouš and P. H. Geubelle, Coupled multi-scale cohesive modeling of failure in heterogeneous adhesives, *Int. J. Numer. Meth. Eng.* **84** (2010) 916–946.
74. H. Lamari, A. Ammar, P. Cartraud, G. Legrain, F. Chinesta and F. Jacquemin, Routes for efficient computational homogenization of nonlinear materials using the proper generalized decompositions, *Arch. Comput. Methods Eng.* **17** (2010) 373–391.
75. F. Larsson and K. Runesson, On two-scale adaptive FE analysis of micro-heterogeneous media with seamless scale-bridging, *Comput. Meth. Appl. Mech. Eng.* **200** (2011) 2662–2674.
76. F. Larsson, K. Runesson and S. Fang, Computational homogenization of uncoupled consolidation in micro-heterogeneous porous media, *Int. J. Numer. Anal. Meth. Geomech.* **34** (2010a) 1431–1458.

77. F. Larsson, K. Runesson and F. Su, Variationally consistent computational homogenization of transient heat flow, *Int. J. Numer. Meth. Eng.* **81** (2010b) 1659–1686.
78. F. Larsson, K. Runesson, S. Saroukhani and R. Vafadari, Computational homogenization based on a weak format of micro-periodicity for RVE-problems, *Comput. Meth. Appl. Mech. Eng.* **200** (2011) 11–26.
79. R. Larsson and S. Diebels, A second-order homogenization procedure for multi-scale analysis based on micropolar kinematics, *Int. J. Numer. Meth. Eng.* **69** (2007) 2485–2512.
80. S. Lee and V. Sundararaghavan, Multi-scale homogenization of moving interface problems with flux jumps: Application to solidification, *Comput. Mech.* **44** (2009) 297–307.
81. M. Lefik, D. P. Boso and B. A. Schrefler, Artificial neural networks in numerical modelling of composites, *Comput. Meth. Appl. Mech. Eng.* **198** (2009) 1785–1804.
82. G. Legrain, P. Cartraud, I. Perreard and N. Moës, An X-FEM and level set computational approach for image-based modelling: Application to homogenization, *Int. J. Numer. Meth. Eng.* **86** (2011) 915–934.
83. F. Lene and D. Leguillon, Homogenized constitutive law for a partially cohesive composite material, *Int. J. Solids Struct.* **18** (1982) 443–458.
84. J. H. Lim, D. Sohn, J. H. Lee and S. Im, Variable-node finite elements with smoothed integration techniques and their applications for multiscale mechanics problems, *Comput. Struct.* **88** (2010) 413–425.
85. C. Linder and F. Armero, Finite elements with embedded strong discontinuities for the modeling of failure in solids, *Int. J. Numer. Meth. Eng.* **72** (2007) 1391–1433.
86. O. Lloberas-Valls, D. J. Rixen, A. Simone and L. J. Sluys, Multiscale domain decomposition analysis of quasi-brittle heterogeneous materials, *Int. J. Numer. Meth. Eng.* (2011), Accepted for publication.
87. S. Loehnert and T. Belytschko, A multiscale projection method for macro/micro-crack simulations, *Int. J. Numer. Meth. Eng.* **71** (2007) 1466–1482.
88. J. Mandel, *Plasticité Classique et Viscoplasticité* (Springer-Verlag, Udine Italy, 1971).
89. T. J. Massart, R. H. J. Peerlings and M. G. D. Geers, A dissipation-based control method for the multi-scale modelling of quasi-brittle materials, *Comptes Rendus Mécanique* **333** (2005) 521–527.
90. T. J. Massart, R. H. J. Peerlings and M. G. D. Geers, An enhanced multi-scale approach for masonry wall computations with localization of damage, *Int. J. Numer. Meth. Eng.* **69** (2007a) 1022–1059.
91. T. J. Massart, R. H. J. Peerlings and M. G. D. Geers, Structural damage analysis of masonry walls using computational homogenization, *Int. J. Damage Mech.* **16** (2007b) 199–226.
92. K. Matouš, M. G. Kulkarni and P. H. Geubelle, Multiscale cohesive failure modeling of heterogeneous adhesives, *J. Mech. Phys. Solids* **56** (2008) 1511–1533.
93. C. McVeigh, F. Vernerey, W. K. Liu and L. C. Brinson, Multiresolution analysis for material design, *Comput. Methods Appl. Mech. Eng.* **195** (2006) 5053–5076.
94. B. C. N. Mercatoris and T. J. Massart, Assessment of periodic homogenisation-based multiscale computational schemes for quasi-brittle structural failure, *Int. J. Multi. Comput. Eng.* **7** (2009) 153–170.
95. B. C. N. Mercatoris and T. J. Massart, A coupled two-scale computational scheme for the failure of periodic quasi-brittle thin planar shells and its application to masonry, *Int. J. Numer. Meth. Eng.* **85** (2011) 1177–1206.

96. B. C. N. Mercatoris, Ph. Bouillard and T. J. Massart, Multi-scale detection of failure in planar masonry thin shells using computational homogenisation, *Eng. Fract. Mech.* **76** (2009) 479–499.
97. S. Mesarovic and J. Padbidri, Minimal kinematic boundary conditions for simulations of disordered microstructures, *Philosophical Magazine* **85** (2005) 65–78.
98. C. Miehe and C. G. Bayreuther, On multiscale FE analyses of heterogeneous structures: From homogenization to multigrid solvers, *Int. J. Numer. Meth. Eng.* **71** (2007) 1135–1180.
99. C. Miehe and A. Koch, Computational micro-to-macro transitions of discretized microstructures undergoing small strains, *Arch. Appl. Mech.* **72** (2002) 300–317.
100. C. Miehe, J. Schröder and J. Schotte, Computational homogenization analysis in finite plasticity simulation of texture development in polycrystalline materials, *Comput. Meth. Appl. Mech. Eng.* **171** (1999) 387–418.
101. C. Miehe, J. Dettmar and D. Zäh, Homogenization and two-scale simulations of granular materials for different microstructural constraints, *Int. J. Numer. Meth. Eng.* **83** (2010) 1206–1236.
102. E. Monteiro, J. Yvonnet and Q. C. He, Computational homogenization for nonlinear conduction in heterogeneous materials using model reduction, *Comput. Mater. Sci.* **42** (2008) 704–712.
103. T. Nakamura and S. Suresh, Effects of thermal residual stresses and fiber packing on deformation of metal-matrix composites, *Acta Metallurgica et Materialia* **41** (1993) 1665–1681.
104. S. Nemat-Nasser and M. Hori, *Micromechanics: Overall Properties of Heterogeneous Materials* (Elsevier, 1999).
105. D. Néron and P. Ladevèze, Proper generalized decomposition for multiscale and multiphysics problems, *Arch. Comput. Meth. Eng.* **17** (2010) 351–372.
106. S. Nezamabadi, J. Yvonnet, H. Zahrouni and M. Potier-Ferry, A multilevel computational strategy for handling microscopic and macroscopic instabilities, *Comput. Meth. Appl. Mech. Eng.* **198** (2009) 2099–2110.
107. V. P. Nguyen, *Multiscale Failure Modelling of Quasi-Brittle Materials*, Ph.D. thesis (Delft University of Technology, 2011).
108. V. P. Nguyen, O. Lloberas Valls, M. Stroeven and L. J. Sluys, On the existence of representative volumes for softening quasi-brittle materials — A failure zone averaging scheme, *Comput. Meth. Appl. Mech. Eng.* **199** (2010) 3028–3038.
109. V. P. Nguyen, O. Lloberas-Valls, M. Stroeven and L. J. Sluys, Homogenization-based multiscale crack modelling: From micro-diffusive damage to macro-cracks, *Comput. Meth. Appl. Mech. Eng.* **200** (2011) 1220–1236.
110. V. P. Nguyen, O. Lloberas-Valls, M. Stroeven and L. J. Sluys, Computational homogenization for multiscale crack modelling, Implementational and computational aspects, *Int. J. Numer. Meth. Eng.* **89** (2012a) 192–226.
111. V. P. Nguyen, M. Stroeven and L. J. Sluys, Multiscale failure modelling of concrete: Micromechanical modelling, discontinuous homogenization and parallel computations, *Comput. Meth. Appl. Mech. Eng.* (2012b) 201–204, 139–156.
112. V. P. Nguyen, M. Stroeven and L. J. Sluys, An enhanced continuous-discontinuous multiscale method for modelling mode-I failure in random heterogeneous quasi-brittle materials, *Eng. Fract. Mech.* **79** (2012c) 78–102.
113. M. Nitka, G. Combe, C. Dascalu and J. Desrues, Two-scale modeling of granular materials: A DEM-FEM approach, *Granular Matter* **13** (2011) 277–281.
114. C. Oskay, Two-level multiscale enrichment methodology for modeling of heterogeneous plates, *Int. J. Numer. Meth. Eng.* **80** (2009) 1143–1170.

115. C. Oskay and J. Fish, On calibration and validation of eigendeformation-based multiscale models for failure analysis of heterogeneous systems, *Comput. Mech.* **42** (2007a) 181–195.
116. C. Oskay and J. Fish, Eigendeformation-based reduced order homogenization for failure analysis of heterogeneous materials, *Comput. Meth. Appl. Mech. Eng.* **196** (2007b) 1216–1243.
117. C. Oskay and G. Pal, A multiscale failure model for analysis of thin heterogeneous plates, *Int. J. Damage Mech.* **19** (2010) 575–610.
118. M. Ostoja-Starzewski, Microstructural randomness versus representative volume element in thermomechanics, *J. Appl. Mech.* **69** (2002) 25–35.
119. I. Özdemir, W. A. M. Brekelmans and M. G. D. Geers, Computational homogenization for heat conduction in heterogeneous solids, *Int. J. Numer. Meth. Eng.* **73** (2008a) 185–204.
120. I. Özdemir, W. A. M. Brekelmans and M. G. D. Geers, FE^2 computational homogenization for the thermo-mechanical analysis of heterogeneous solids, *Comput. Meth. Appl. Mech. Eng.* **198** (2008b) 602–613.
121. C. Pelissou, J. Baccou, Y. Monerie and F. Perales, Determination of the size of the representative volume element for random quasi-brittle composites, *Int. J. Solids Struct.* **46** (2009) 2842–2855.
122. D. Perić, E. A. de Souza Neto, R. A. Feijóo, M. Partovi and A. J. C. Molina, On micro-to-macro transitions for multi-scale analysis of non-linear heterogeneous materials: Unified variational basis and finite element implementation, *Int. J. Numer. Meth. Eng.* **87** (2011) 149–170.
123. H. E. Pettermann and S. Suresh, A comprehensive unit cell model: A study of coupled effects in piezoelectric 1–3 composites, *Int. J. Solids Struct.* **37** (2000) 5447–5464.
124. P. Raghavan and S. Ghosh, A continuum damage mechanics model for unidirectional composites undergoing interfacial debonding, *Mech. Mater.* **37** (2005) 955–979.
125. Rahul and S. De, An efficient coarse-grained parallel algorithm for global-local multiscale computations on massively parallel systems, *Int. J. Numer. Meth. Eng.* **82** (2010) 379–402.
126. S. Ricker, J. Mergheim and P. Steinmann, On the multiscale computation of defect driving forces, *Int. J. Multi. Comput. Eng.* **7** (2009) 457–474.
127. S. Ricker, J. Mergheim, P. Steinmann and R. Müller, A comparison of different approaches in the multi-scale computation of configurational forces, *Int. J. Fract.* **166** (2010) 203–214.
128. J. Schröder and M. A. Keip, A framework for the two-scale homogenization of electromechanically coupled boundary value problems, *Computer Methods in Mechanics*, Vol. 1, eds. M. Kuczma and K. Wilmanski (Springer Berlin Heidelberg, Berlin, Heidelberg, 2010), pp. 311–329.
129. G. K. Sfantos and M. H. Aliabadi, Multi-scale boundary element modelling of material degradation and fracture, *Comput. Meth. Appl. Mech. Eng.* **196** (2007) 1310–1329.
130. R. J. M. Smit, W. A. M. Brekelmans and H. E. H. Meijer, Prediction of the mechanical behavior of nonlinear heterogeneous systems by multi-level finite element modeling, *Comput. Meth. Appl. Mech. Eng.* **55** (1998) 181–192.
131. D. D. Somer, E. A. de Souza Neto, W. G. Dettmer and D. Perić, A sub-stepping scheme for multi-scale analysis of solids, *Comput. Meth. Appl. Mech. Eng.* **198** (2009) 1006–1016.
132. J. H. Song and T. Belytschko, Multiscale aggregating discontinuities method for micro-macro failure of composites, *Comp. Part B: Eng.* **40** (2009) 417–426.

133. F. V. Souza and D. H. Allen, Multiscale modeling of impact on heterogeneous viscoelastic solids containing evolving microcracks, *Int. J. Numer. Meth. Eng.* **82** (2010) 464–504.
134. F. V. Souza and D. H. Allen, Modeling the transition of microcracks into macrocracks in heterogeneous viscoelastic media using a two-way coupled multiscale model, *Int. J. Solids Struct.* **48** (2011) 3160–3175.
135. F. V. Souza, D. H. Allen and Y.-R. Kim, Multiscale model for predicting damage evolution in composites due to impact loading, *Compos. Sci. Technol.* **68** (2008) 2624–2634.
136. M. Stroeven, H. Askes and L. J. Sluys, Numerical determination of representative volumes for granular materials, *Comput. Meth. Appl. Mech. Eng.* **193** (2004) 3221–3238.
137. P. M. Suquet, Local and global aspects in the mathematical theory of plasticity, *Plasticity Today: Modelling, Methods and Applications*, eds. A. Sawczuk and G. Bianchi (London, Elsevier, 1985), pp. 279–310.
138. S. Swaminathan and S. Ghosh, Statistically equivalent representative volume elements for unidirectional composite microstructures: Part II — with interfacial debonding, *J. Compos. Mater.* **40** (2006) 605–621.
139. S. Swaminathan, S. Ghosh and N. J. Pagano, Statistically equivalent representative volume elements for unidirectional composite microstructures: Part I — without damage, *J. Compos. Mater.* **40** (2006) 583–604.
140. I. Temizer and P. Wriggers, An adaptive multiscale resolution strategy for the finite deformation analysis of microheterogeneous structures, *Comput. Meth. Appl. Mech. Eng.* **200** (2011) 2639–2661.
141. I. Temizer and T. I. Zohdi, A numerical method for homogenization in non-linear elasticity, *Comput. Mech.* **40** (2006) 281–298.
142. K. Terada, M. Hori, T. Kyoya and N. Kikuchi, Simulation of the multi-scale convergence in computational homogenization approaches, *Int. J. Solids Struct.* **37** (2000) 2285–2311.
143. J. M. Tyrus, M. Gosz and E. DeSantiago, A local finite element implementation for imposing periodic boundary conditions on composite micromechanical models, *Int. J. Solids Struct.* **44** (2007) 2972–2989.
144. J. F. Unger and C. Könke, Coupling of scales in a multiscale simulation using neural networks, *Comput. Struct.* **86** (2008) 1994–2003.
145. J. F. Unger and C. Könke, Neural networks as material models within a multiscale approach, *Comput. Struct.* **87** (2009) 1177–1186.
146. O. van der Sluis, P. J. G. Schreurs, W. A. M. Brekelmans and H. E. H. Meijer, Overall behaviour of heterogeneous elastoviscoplastic materials: Effect of microstructural modelling, *Mech. Mater.* **32** (2000) 449–462.
147. C. V. Verhoosel, J. J. C. Remmers and M. A. Gutiérrez, A dissipation-based arc-length method for robust simulation of brittle and ductile failure, *Int. J. Numer. Meth. Eng.* **77** (2009a) 1290–1321.
148. C. V. Verhoosel, J. J. C. Remmers and M. A. Gutiérrez, A partition of unity-based multiscale approach for modelling fracture in piezoelectric ceramics, *Int. J. Numer. Meth. Eng.* (2009b).
149. C. V. Verhoosel, J. J. C. Remmers, M. A. Gutiérrez and R. de Borst, Computational homogenisation for adhesive and cohesive failure in quasi-brittle solids, *Int. J. Numer. Meth. Eng.* **83** (2010) 1155–1179.

150. F. J. Vernerey, W. K. Liu, B. Moran and G. Olson, A micromorphic model for the multiple scale failure of heterogeneous materials, *J. Mech. Phys. Solids* **56** (2008) 1320–1347.
151. F. J. Vernerey, W. K. Liu, B. Moran and G. Olson, Multi-length scale micromorphic process zone model, *Comput. Mech.* **44** (2009) 433–445.
152. J. F. Vernerey, W. K. Liu and B. Moran, Multi-scale micromorphic theory for hierarchical materials, *J. Mech. Phys. Solids* **55** (2007) 2603–2651.
153. C. Wellmann and P. Wriggers, A two-scale model of granular materials, *Comput. Meth. Appl. Mech. Eng.* in Press, Corrected Proof. doi:10.1016/j.cma.2010.12.023.
154. G. N. Wells and L. J. Sluys, A new method for modelling cohesive cracks using finite elements, *Int. J. Numer. Meth. Eng.* **50** (2001) 2667–2682.
155. L. Wiechert and W. A. Wall, A nested dynamic multi-scale approach for 3D problems accounting for micro-scale multi-physics, *Comput. Meth. Appl. Mech. Eng.* **199** (2010) 1342–1351.
156. X. P. Xu and A. Needleman, Numerical simulations of fast crack growth in brittle solids, *J. Mech. Phys. Solids* **42** (1994) 1434, 1397.
157. Z. Yuan and J. Fish, Toward realization of computational homogenization in practice, *Int. J. Numer. Meth. Eng.* **73** (2008) 361–380.
158. Z. Yuan and J. Fish, Multiple scale eigendeformation-based reduced order homogenization, *Comput. Meth. Appl. Mech. Eng.* **198** (2009) 2016–2038.
159. G. J. Yun, J. Ghaboussi and A. S. Elnashai, A new neural networkbased model for hysteretic behavior of materials, *Int. J. Numer. Meth. Eng.* **73** (2008) 447–469.
160. J. Yvonnet and Q.-C. He, The reduced model multiscale method (R3M) for the nonlinear homogenization of hyperelastic media at finite strains, *J. Comput. Phys.* **223** (2007) 341–368.
161. J. Yvonnet, D. Gonzalez and Q.-C. He, Numerically explicit potentials for the homogenization of nonlinear elastic heterogeneous materials, *Comput. Meth. Appl. Mech. Eng.* **198** (2009) 2723–2737.
162. T. I. Zohdi and P. Wriggers, *Introduction to Computational Micromechanics*, Lecture Notes in Applied and Computational Mechanics, Vol. 20 (Springer, Berlin, 2005).
163. T. I. Zohdi, J. T. Oden and G. J. Rodin, Hierarchical modeling of heterogeneous bodies, *Comput. Meth. Appl. Mech. Eng.* **138** (1996) 273–298.